

1           **Multi-omics analysis of multiple glucose-sensing receptor systems in yeast**

2

3

4   Shuang Li<sup>1</sup>, Yuanyuan Li<sup>2</sup>, Blake R. Rushing<sup>2</sup>, Sarah E. Harris<sup>3</sup>, Susan L. McRitchie<sup>2</sup>, Daniel  
5   Dominguez<sup>1</sup>, Susan J. Sumner<sup>2</sup>\*, and Henrik G. Dohlman<sup>1</sup>\*

6

7   <sup>1</sup> Department of Pharmacology, University of North Carolina at Chapel Hill, Chapel Hill, North  
8   Carolina, USA

9

10   <sup>2</sup> Nutrition Research Institute, Department of Nutrition, School of Public Health, University of  
11   North Carolina at Chapel Hill, Chapel Hill, North Carolina, USA

12

13   <sup>3</sup> Department of Biochemistry and Biophysics, University of North Carolina at Chapel Hill,  
14   Chapel Hill, North Carolina, USA

15

16

17   \*[hdohlman@med.unc.edu](mailto:hdohlman@med.unc.edu) (H.G.D.); [susan\\_sumner@unc.edu](mailto:susan_sumner@unc.edu) (S.J.S.)

18

19   Key words: metabolomics, transcriptomics, G protein-coupled receptor, transceptor, G protein,  
20   RAS, glucose, yeast

21

22   Short title: Glucose receptors in yeast

23

## 24 **ABSTRACT**

25 The yeast *Saccharomyces cerevisiae* has long been used to produce alcohol from glucose and  
26 other sugars. While much is known about glucose metabolism, relatively little is known about  
27 the receptors and signaling pathways that indicate glucose availability. Here we compare the  
28 two glucose receptor systems in *S. cerevisiae*. The first is a heterodimer of transporter-like  
29 proteins (transceptors), while the second is a seven-transmembrane receptor coupled to a large  
30 G protein (Gpa2) and two small G proteins (Ras1 and Ras2). Through comprehensive  
31 measurements of glucose-dependent transcription and metabolism, we demonstrate that the  
32 two receptor systems have distinct roles in glucose signaling: the G protein-coupled receptor  
33 directs carbohydrate and energy metabolism, while the transceptors regulate ancillary  
34 processes such as ribosome, amino acids, cofactor and vitamin metabolism. The large G  
35 protein transmits the signal from its cognate receptor, while the small G protein Ras2 (but not  
36 Ras1) integrates responses from both receptor pathways. Collectively, our analysis reveals the  
37 molecular basis for glucose detection and the earliest events of glucose-dependent signal  
38 transduction in yeast.

39

## 40 **INTRODUCTION**

41 Most eukaryotic organisms use glucose as the principal source of carbon and energy.  
42 Changes in glucose availability result in important metabolic and transcriptional changes that  
43 dictate the transition between respiratory and fermentative metabolism [1-4]. Among the best  
44 understood systems is that of the yeast *Saccharomyces cerevisiae* (meaning “sugar fungus”  
45 and “beer”). Biochemical studies of yeast fermentation led to the discovery of enzymes  
46 (meaning “in yeast”) and the founding of biochemistry as a distinct scientific discipline.

47 While the details of glucose metabolism are well understood, we know comparatively  
48 little about changes in signal transduction and cellular metabolism in response to glucose  
49 availability. These include changes attributed to glucose binding to cell surface receptors and

50 activation of signaling pathways immediately downstream of the receptor but upstream of  
51 glycolysis. In this instance, an increase in glucose is transmitted by two distinct processes (Fig  
52 1). In the first, glucose is detected by a G protein-coupled receptor (GPCR) known as Gpr1 and  
53 transmitted through G protein  $\alpha$  and  $\beta$  subunits, named Gpa2 and Asc1 respectively [5-13]. This  
54 in turn activates the small G proteins Ras1 and Ras2, through the action of guanine nucleotide  
55 exchange factors [14-20]. In contrast to *ras2* however, *ras1* has no observed phenotype under  
56 standard laboratory growth conditions [21]. Collectively [22-33], these proteins activate the  
57 effector enzyme adenylyl cyclase [24, 34-36] leading to an increase in cellular cAMP [9, 26, 37].  
58 This second messenger binds directly to protein kinase A, which goes on to phosphorylate  
59 multiple intracellular proteins involved in glucose uptake, metabolism and storage [38-44].

60

61 **Fig 1. Glucose-sensing pathways in yeast.** Two receptor pathways in *S. cerevisiae* respond to  
62 glucose availability. Gpr1 transmits its signal through the large G protein Gpa2 [5-7, 9-11], as well  
63 as the small G proteins Ras1 and Ras2. The transceptors Snf3 and Rgt2 recruit the protein  
64 kinases Yck1 and Yck2 as well as the transcription corepressors Mth1 and Std1 [45-49]. GPCR:  
65 G protein coupled receptor; GAP: GTPase activating protein; GEF: guanine nucleotide exchange  
66 factor; AC: adenylyl cyclase; PDE: phosphodiesterase; TF: transcription factor; CKI: casein kinase  
67 I; PKA: protein kinase A.

68

69 The second glucose-sensing system consists of the cell surface proteins Snf3 and Rgt2.  
70 Although they resemble glucose transporters, Snf3 and Rgt2 appear to have lost their  
71 transporter function and instead serve exclusively as receptor or “transceptor” proteins.  
72 Following glucose addition [45-47], Snf3 and Rgt2 recruit the Type I casein kinases Yck1 and  
73 Yck2 as well as the transcription corepressors Mth1 and Std1 [48, 49]. Subsequent  
74 phosphorylation of these factors results in their ubiquitination and degradation [50-52]; this

75 derepresses genes encoding hexose transporters and promotes the uptake of the newly  
76 available sugars [47, 53-62].

77 Here, we compare the function of the two glucose signaling pathways. In particular, we  
78 employ transcriptomics and metabolomics to provide a comprehensive view of the cellular  
79 response to glucose. Our analysis reveals new and complementary functions for the two  
80 glucose sensing receptors and an unexpected role for Ras2 as an integrator of these two  
81 receptor pathways.

82

## 83 **RESULTS**

84 *Unsupervised Principal Component Analysis (PCA)*. It is well established that yeast  
85 employs two different receptor systems in response to glucose. To investigate the impact of  
86 each receptor system, we used untargeted transcriptomics and metabolomics on wildtype cells  
87 and mutants lacking the GPCR Gpr1, the large G protein Gpa2, the small G proteins Ras1 or  
88 Ras2, or the transceptors Snf3 and Rgt2, under high or low glucose conditions. Log phase  
89 wildtype and mutant cells (all prototrophic) were grown for 1 hour in low (L, 0.05%) glucose,  
90 then divided and either left untreated or treated with high (H, 2%) glucose for 2 minutes  
91 (metabolomics) or 10 minutes (transcriptomics). These time points were selected based on prior  
92 data, showing an early and transient spike of cAMP and a subsequent induction of genes within  
93 10 minutes of glucose treatment [1, 13].

94 Principal Component Analysis (PCA) is an unsupervised multivariate analysis method  
95 useful for the visualization of the relationship between observations and variables. When  
96 applied to our transcriptomics data, PCA revealed good differentiation based on the proximity of  
97 data points for a given treatment and genotype (S1A Fig). This analysis revealed that PC1,  
98 which aligns primarily with treatment, accounts for 89% of variance while PC2, which aligns  
99 primarily with genotype, represents 4% of variance. Thus, the first 2 components explained 93%  
100 of the variance. For metabolomics, the first 2 components explained 50% of the variance (S1B

101 Fig). With the exception of *ras1*, the mutants were distant from wildtype in both measurements.  
102 While *gpr1* aligned closely with *gpa2*, *snf3 rgt2* was on the opposite side of wildtype. The *ras2*  
103 mutant was located between the two receptor mutants. These measures indicate distinct effects  
104 of the two receptor systems, and a potential role for Ras2 in both.

105

## 106 **Glucose sensing in wildtype cells.**

107         Glucose has multiple and complex effects on metabolism and gene expression. To  
108 validate our approach, we first performed pathway enrichment analysis, comparing high and low  
109 glucose in wildtype cells. For transcriptomics we used the ClusterProfiler package in R [63] and  
110 performed gene set enrichment analysis (GSEA) with the Kyoto Encyclopedia of Genes and  
111 Genomes (KEGG) database [64-66]. As expected, perturbed pathways were mainly associated  
112 with carbohydrate, amino acids, lipids and nucleotide metabolism as well as transcription,  
113 ribosome, replication, and cell cycle pathways (See Table 1 in [13], reproduced in S1 Table).  
114 These pathways are important for cell growth following the addition of glucose [67]. For  
115 metabolomics we used MetaboAnalystR, which integrates the results of Mummichog and  
116 GSEA, to produce the combined p-values reported for each pathway (See Table 1 in [13]  
117 reproduced in S1 Table) [68-70]. We identified enrichment in six pathways associated with  
118 metabolism of carbohydrates, amino acids, and lipids, which is consistent with our  
119 transcriptomics analysis. Below we elaborate on how the two receptor systems function  
120 individually and in relation to one another.

121

## 122 **Comparison of glucose signaling by the GPCR and transceptor systems.**

123         *Transcriptomics analysis.* We next determined the transcriptional response to high  
124 glucose, comparing wildtype cells with mutants lacking the GPCR (*gpr1*), or the two  
125 transceptors (*snf3 rgt2*). In comparison to wildtype, *gpr1* affected pathways related to oxidative  
126 phosphorylation as well as starch and sucrose metabolism, both of which are centered on

127 carbohydrate utilization and energy metabolism (Tables 1 and S2). In comparison to wildtype,  
 128 *snf3 rgt2* affected pathways related to RNA polymerase, ribosome, autophagy and amino acid  
 129 metabolism, which are centered on nitrogen utilization and translation (Tables 2 and S3). Thus,  
 130 under high glucose conditions, the GPCR and transceptor pathways primarily regulate  
 131 carbohydrate and amino acid metabolism, respectively.

132  
 133 **Table 1. Single- and multi-omics integration results for *gpr1*.** First block shows GSEA for  
 134 transcriptomics with adjusted p-value <0.05, arranged in ascending order; second block shows  
 135 MetaboAnalystR pathway enrichment analysis for metabolomics with combined p-value <0.05,  
 136 arranged in ascending order; third block shows MetaboAnalystR joint pathway analysis with  
 137 adjusted p-value <0.05, arranged in ascending order, as detailed in Methods.

138

Transcriptomics		Metabolomics		Integration	
enriched pathways	adjusted p-value	enriched pathways	combined p-value	enriched pathways	adjusted p-value
Oxidative phosphorylation	0.0082	Fructose and mannose metabolism	0.0021	Oxidative phosphorylation	5.24E-19
Starch and sucrose metabolism	0.0082	Purine metabolism	0.0034	Galactose metabolism	8.60E-13
		Amino sugar and nucleotide sugar metabolism	0.0075	Starch and sucrose metabolism	6.56E-10
		Galactose metabolism	0.0075	ABC transporters	7.22E-08
		Tyrosine metabolism	0.0090	Glycolysis or Gluconeogenesis	1.75E-07
		Glutathione metabolism	0.0107	Arginine biosynthesis	5.76E-05
		Lysine biosynthesis	0.0177	Alanine, aspartate and glutamate metabolism	0.0001
		Arginine biosynthesis	0.0229	Purine metabolism	0.0001
		Butanoate metabolism	0.0375	Citrate cycle (TCA cycle)	0.0001

				Fructose and mannose metabolism	0.0003
				Amino sugar and nucleotide sugar metabolism	0.0009
				Cysteine and methionine metabolism	0.0025
				Pentose phosphate pathway	0.0025
				Nitrogen metabolism	0.0128
				beta-Alanine metabolism	0.0128
				Glycine, serine and threonine metabolism	0.0175
				Pyruvate metabolism	0.0264
				Glutathione metabolism	0.0266

139

140 **Table 2. Single- and multi-omics integration results for *snf3 rgt2*.** First block shows GSEA  
 141 for transcriptomics with adjusted p-value <0.05, arranged in ascending order; second block shows  
 142 MetaboAnalystR pathway enrichment analysis for metabolomics with combined p-value <0.05,  
 143 arranged in ascending order; third block shows MetaboAnalystR joint pathway analysis with  
 144 adjusted p-value <0.05, arranged in ascending order, as detailed in Methods.

145

Transcriptomics		Metabolomics		Integration	
enriched pathways	adjusted p-value	enriched pathways	combined p-value	enriched pathways	adjusted p-value
Ribosome	0.0076	Purine metabolism	0.0005	Ribosome	1.12E-74
Ribosome biogenesis in eukaryotes	0.0076	Arginine biosynthesis	0.0026	Purine metabolism	1.76E-09
Sulfur metabolism	0.0076	Cysteine and methionine metabolism	0.0027	Longevity regulating pathway	9.20E-06

RNA polymerase	0.0154	Glyoxylate and dicarboxylate metabolism	0.0055	Alanine, aspartate and glutamate metabolism	2.05E-05
Nitrogen metabolism	0.0165	Glycine, serine and threonine metabolism	0.0085	Arginine biosynthesis	0.0004
Autophagy	0.0165	Taurine and hypotaurine metabolism	0.0172	Glycine, serine and threonine metabolism	0.0006
Alanine, aspartate and glutamate metabolism	0.0289	Glutathione metabolism	0.0174	Glycolysis or Gluconeogenesis	0.0049
Proteasome	0.0465	Methane metabolism	0.0254	Starch and sucrose metabolism	0.0080
				Cysteine and methionine metabolism	0.0088
				One carbon pool by folate	0.0174
				Glyoxylate and dicarboxylate metabolism	0.0174
				Sulfur metabolism	0.0193
				Pyruvate metabolism	0.0193
				Histidine metabolism	0.0193
				Galactose metabolism	0.0261
				Peroxisome	0.0295
				Glycerolipid metabolism	0.0392

146

147 **Fig 2. Comparing differentially expressed genes (DEGs) of *gpr1* and *snf3 rgt2*.** A) Venn  
 148 diagram of subsets of DEGs, for *gpr1* vs. wildtype and *snf3 rgt2* vs. wildtype, after glucose addition  
 149 to 2%. Upper semicircle shows up-regulated DEGs and lower semicircle shows down-regulated  
 150 DEGs. Numbers in the overlapping region are shared DEGs regulated in the same direction.  
 151 Numbers in parenthesis are shared DEGs regulated in the opposite direction, and are placed in  
 152 the area corresponding to the direction of regulation. DEGs used for ORA analysis that are B)  
 153 unique to *gpr1*; C) unique to *snf3 rgt2*; D) shared and change in the same direction; E) shared



154 and change in the opposite direction. Listed are all pathways and their functional categories with  
155 adjusted p-value <0.05.

156

157 We then performed over-representation analysis (ORA) for differentially expressed  
158 genes (DEGs), comparing *gpr1* vs. wildtype and *snf3 rgt2* vs. wildtype, both under high glucose  
159 conditions. In each case we defined the DEGs as having an adjusted p-value <0.05, absolute  
160 log<sub>2</sub> fold-change value >1 and baseMean >100. Whereas GSEA is a type of functional class  
161 scoring that considers a complete list of ranked items (all gene transcripts in this application),  
162 ORA considers a thresholded subset of items (DEGs, defined above). In this way, we were able  
163 to gain a detailed understanding of how the mutants are similar and how they differ from one  
164 another. Fig 2A shows a Venn diagram comparing the specific DEGs for each mutant vs. the  
165 wildtype strain (S4 Table). As shown in Fig 2B, DEGs unique to *gpr1* were primarily related to  
166 carbohydrate and energy metabolism, consistent with Gpr1's function as a sensor of glucose  
167 availability. DEGs unique to *snf3 rgt2* were mainly related to ribosome, purine, cofactor and  
168 vitamin metabolism (Fig 2C). While the two mutant strains had concordant effects on some  
169 DEGs (Fig 2D), they had - contrary to our expectations - substantial and opposing effects on a  
170 broad set of DEGs primarily related to carbohydrate and amino acid metabolism (Fig 2E). Thus,  
171 GSEA and ORA are in agreement, and indicate that the two receptor pathways are largely  
172 distinct. When the pathways converge on a shared set of carbohydrate- and amino acid-related  
173 transcripts (DEGs), they do so largely in opposition to one another.

174 *Metabolomics analysis.* Gene transcription is regulated by, and in turn regulates,  
175 complex metabolic processes in the cell. To better understand the relationship of these two  
176 glucose-sensing systems, we examined the role of each receptor type after glucose addition,  
177 and did so using untargeted metabolomics. Based on MetaboAnalystR, our mass spectrometry  
178 data show that the *gpr1* cells were enriched in nine pathways related to carbohydrate and amino  
179 acid metabolism (Tables 1 and S2), while *snf3 rgt2* cells were enriched in eight pathways,

180 including those related to amino acid and purine metabolism, but not central carbohydrate  
181 metabolism (Tables 2 and S3). A Venn diagram shows shared and unique metabolites that were  
182 significantly perturbed in each strain (Fig 3A and S5 Table). Values were obtained from the  
183 output of MetaboAnalystR and represent annotations with adjusted p-value <0.05. These are  
184 hereafter referred to as significantly perturbed metabolites (SPMs). ORA revealed that several  
185 purine metabolites changed in the same direction (Fig 3B) while a substantial number of  
186 carbohydrate metabolites changed in the opposite direction (Fig 3C). As expected, the signals  
187 identified and annotated by MetaboAnalyst mirror those obtained using in-house library  
188 annotation, developed with data acquired for standards run under the same conditions as the  
189 study samples, as well as matching to public databases (PD), as described in our companion  
190 manuscript [13], and reported in S6 Table. Subsequent analysis relied on MetaboAnalystR,  
191 which is well suited for annotating a large number of signals.

192

193 **Fig 3. Comparing significantly perturbed metabolites (SPMs) of *gpr1* and *snf3 rgt2*.** A) Venn  
194 diagram of subsets of SPMs, for *gpr1* vs. wildtype and *snf3 rgt2* vs. wildtype, after glucose  
195 addition. Upper semicircle shows up-regulated SPMs and lower semicircle shows down-regulated  
196 SPMs. Numbers in the overlapping region are shared SPMs regulated in the same direction.  
197 Numbers in parenthesis are shared SPMs regulated in the opposite direction, and are placed in  
198 the area corresponding to the direction of regulation. SPMs used for ORA analysis that are B)  
199 shared and change in the same direction; C) shared and change in the opposite direction. Listed  
200 are all pathways and their functional categories with adjusted p-value <0.05.

201

202 *Integration analysis.* Our analysis above shows that the GPCR Gpr1 regulates  
203 carbohydrate metabolism while the transceptors Snf3 and Rgt2 regulate ribosome, amino acid,  
204 cofactor and vitamin metabolism. Effects that are shared but opposing are primarily related to  
205 carbohydrate metabolism; however, these represent only a small subset of the DEGs and SPMs

206 affected by Snf3 and Rgt2. In general, and to our surprise, the glucose transceptors did little to  
207 regulate the metabolism of glucose and other sugars. To gain a deeper understanding of the  
208 functional relationship between changes in gene transcription and host metabolites, we  
209 employed the joint pathway analysis module in MetaboAnalystR, as described previously [13,  
210 69, 70]. In this application, we input all DEGs (transcriptomics) and SPMs (metabolomics) and  
211 queried for those over-represented in KEGG. By integrating the data in this manner, we  
212 increased the power of our analysis and were able to obtain more information than could be  
213 gleaned from transcriptomics or metabolomics alone. Once again, we found that Gpr1 primarily  
214 regulates carbohydrate and energy metabolism (Tables 1 and S2) while Snf3 and Rgt2 primarily  
215 regulate the ribosome, amino acids, lipids and cofactor metabolism (Tables 2 and S3). Both  
216 receptor systems affect genes or metabolites involved in carbohydrates, amino acids and purine  
217 metabolites. Thus integration analysis confirms what we observed on the single-omics level:  
218 Gpr1 is primarily dedicated to carbohydrate metabolism while Snf3 and Rgt2 work to coordinate  
219 other species in response to glucose addition.

220 To visualize the functional relationship of the two receptor systems, we projected the  
221 inputs of our integration analysis onto the pertinent yeast metabolic pathways in KEGG. From  
222 this projection it was evident that the two receptor types regulate distinct and complementary  
223 processes. Specifically, Gpr1 affects pathways related to carbohydrate metabolism and, within  
224 those pathways, a larger number of genes and metabolites compared to Snf3 and Rgt2 (Figs 4A  
225 and S2 and Tables 1 and 2). On the other hand, Snf3 and Rgt2 affect pathways related to  
226 amino acids and, within those pathways, affect a far greater number of genes and metabolites in  
227 comparison to Gpr1 (Figs 4B and S3 and Tables 1 and 2). As presented from the single-omics  
228 analysis above, the shared effects on carbohydrate and amino acids were mostly antagonistic  
229 while the shared effects on purines were concordant.

230

231 **Fig 4. KEGG pathways regulated by *GPR1* or *SNF3* and *RGT2*.** Regions of interest in the  
232 KEGG pathway are shown with genes displayed as rectangles and metabolites displayed as  
233 circles. KEGG compound name for each metabolite is labeled beside the circle. Standard gene  
234 names are labeled inside the rectangle. For enzyme complexes, the gene name for the major  
235 component is shown followed with an ellipsis. The directions of irreversible enzymatic reactions  
236 are shown by the arrows. Reversible reactions are connected by straight lines. DEGs and SPMs  
237 are highlighted in red (*gpr1*) and blue (*snf3 rgt2*). Shared DEGs and SPMs are colored half red  
238 and half blue. A) as compared with *snf3 rgt2*, *gpr1* affected more components in citrate cycle  
239 (TCA cycle, functional category: carbohydrate); B) as compared with *gpr1*, *snf3 rgt2* affected more  
240 components in alanine, aspartate and glutamate metabolism (showing aspartate and glutamate  
241 specifically, functional category: amino acid).

242

243 In summary, our transcriptomics and metabolomics pipeline established a distinct role  
244 for each receptor. Two minutes after sugar addition the GPCR and transceptors have opposing  
245 effects on many of the same metabolites (Fig 3). After ten minutes however, they confer  
246 changes on a largely different set of gene transcripts (Fig 2): whereas the effects of Gpr1 are  
247 mostly limited to genes controlling carbohydrate metabolism, Snf3 and Rgt2 affect more diverse  
248 species, including genes that are related to amino acids, lipids, ribosome, cofactors and  
249 vitamins. Snf3 and Rgt2 do little to alter carbohydrate metabolism, and any changes that do  
250 occur are largely in opposition to Gpr1. Such antagonistic effects may allow the cell to fine tune  
251 responses and to optimize temporal control of enzyme activities.

252

### 253 **Comparison of glucose signaling through large and small G proteins.**

254 Gpr1 acts through a G protein comprised of an  $\alpha$  subunit Gpa2 and an atypical G $\beta$   
255 subunit Asc1 [6-9, 12]. Gpa2 in turn activates the small G proteins Ras1 and Ras2, through the  
256 action of guanine nucleotide exchange factors [14-20]. Our recent analysis of Gpa2 and Asc1

257 revealed that they have mostly opposing effects on transcripts and metabolites. When the  
258 effects are congruent however, they mirror those observed for their shared activator Gpr1 [13].  
259 To better understand how the receptors transmit their signals in response to glucose addition,  
260 we next compared the function of the large and small G proteins (Gpa2, Ras1 and Ras2) using  
261 the same analytical pipeline as described above.

262 *Transcriptomics Analysis.* We began by determining the transcriptional profiles of  
263 individual gene deletion mutants by GSEA, as described above. The *ras1* mutant yielded no  
264 DEGs, consistent with the lack of phenotype for *ras1* in standard laboratory growth conditions  
265 [21]. As shown in Tables 3 and 4 (also S7 and S8 Tables), the *gpa2* mutant affected pathways  
266 related to oxidative phosphorylation and ribosome biogenesis. These pathways were likewise  
267 regulated by *ras2*. In addition, *ras2* affected RNA polymerase, carbohydrate metabolism and  
268 autophagy (Table 4). Overlap between the large and small G proteins was expected given that  
269 both are activated by Gpr1 and both are activators of adenylyl cyclase. However, based on the  
270 Venn diagram, these mutants had correspondent effects on only a small number of genes and  
271 opposing effects on even fewer (Fig 5A and S9 Table). Based on ORA, for the small number of  
272 shared DEGs, *gpa2* and *ras2* had mostly concordant effects on processes related to  
273 carbohydrate, amino acid and lipid metabolism (Fig 5B). DEGs unique to *ras2* affected a broad  
274 spectrum of processes, encompassing all major species in KEGG, including the metabolism of  
275 energy, carbohydrates, amino acids, nucleotides, lipids, cofactors and vitamins (Fig 5C). In  
276 contrast, DEGs unique to *gpa2* affected a small number of processes, related to carbohydrate,  
277 energy and lipid metabolism (Fig 5D). Thus, upon glucose addition, Gpa2 regulates  
278 carbohydrates and lipids, while Ras2 affects all major categories of metabolic processes.

279

280 **Table 3. Single- and multi-omics integration results for *gpa2*.** First block shows GSEA for  
281 transcriptomics with adjusted p-value <0.05, arranged in ascending order; second block shows  
282 MetaboAnalystR pathway enrichment analysis for metabolomics with combined p-value <0.05,

283 arranged in ascending order; third block shows MetaboAnalystR joint pathway analysis with  
 284 adjusted p-value <0.05, arranged in ascending order, as detailed in Methods.  
 285

Transcriptomics		Metabolomics		Integration	
enriched pathways	adjusted p-value	enriched pathways	combined p-value	enriched pathways	adjusted p-value
Ribosome biogenesis in eukaryotes	0.0084	Purine metabolism	0.0021	Oxidative phosphorylation	3.13E-14
Oxidative phosphorylation	0.0084	Fructose and mannose metabolism	0.0047	Galactose metabolism	1.60E-11
		Amino sugar and nucleotide sugar metabolism	0.0079	ABC transporters	1.31E-08
		Galactose metabolism	0.0079	Glycolysis or Gluconeogenesis	8.02E-05
		Glutathione metabolism	0.0155	Fructose and mannose metabolism	8.18E-05
		Tyrosine metabolism	0.0224	Starch and sucrose metabolism	8.18E-05
		Arginine biosynthesis	0.0234	Arginine biosynthesis	0.0012
		Biotin metabolism	0.0252	Pentose phosphate pathway	0.0012
		Aminoacyl-tRNA biosynthesis	0.0360	Purine metabolism	0.0017
		Starch and sucrose metabolism	0.0396	Amino sugar and nucleotide sugar metabolism	0.0073
		Phosphatidylinositol signaling system	0.0424	beta-Alanine metabolism	0.0119
				Alanine, aspartate and glutamate metabolism	0.0139
				Cysteine and methionine metabolism	0.0149
				Citrate cycle (TCA cycle)	0.0221

286

287 **Table 4. Single- and multi-omics integration results for *ras2*.** First block shows GSEA for  
 288 transcriptomics with adjusted p-value <0.05, arranged in ascending order; second block shows  
 289 MetaboAnalystR pathway enrichment analysis for metabolomics with combined p-value <0.05,  
 290 arranged in ascending order; third block shows MetaboAnalystR joint pathway analysis with  
 291 adjusted p-value <0.05, arranged in ascending order, as detailed in Methods.  
 292

Transcriptomics		Metabolomics		Integration	
enriched pathways	adjusted p-value	enriched pathways	combined p-value	enriched pathways	adjusted p-value
Starch and sucrose metabolism	0.0065	Lysine biosynthesis	1.00E-05	Galactose metabolism	1.24E-15
Oxidative phosphorylation	0.0065	Glyoxylate and dicarboxylate metabolism	0.0005	Starch and sucrose metabolism	1.68E-11
Ribosome biogenesis in eukaryotes	0.0065	Glycine, serine and threonine metabolism	0.0009	Glycolysis or Gluconeogenesis	6.26E-08
Ribosome	0.0065	Arginine biosynthesis	0.0017	Glycine, serine and threonine metabolism	4.30E-06
RNA polymerase	0.0092	Cysteine and methionine metabolism	0.0028	ABC transporters	1.03E-05
Galactose metabolism	0.0169	Taurine and hypotaurine metabolism	0.0043	Pentose phosphate pathway	2.27E-05
Autophagy	0.0169	Amino sugar and nucleotide sugar metabolism	0.0043	Cysteine and methionine metabolism	2.27E-05
Meiosis	0.0332	Galactose metabolism	0.0043	Fructose and mannose metabolism	0.0002
Spliceosome	0.0458	Butanoate metabolism	0.0095	Amino sugar and nucleotide sugar metabolism	0.0002
		Lysine degradation	0.0098	Arginine biosynthesis	0.0003
		Aminoacyl-tRNA biosynthesis	0.0098	Purine metabolism	0.0005
		Starch and sucrose metabolism	0.0204	Glyoxylate and dicarboxylate metabolism	0.0009

		Alanine, aspartate and glutamate metabolism	0.0372	Peroxisome	0.0014
		Fructose and mannose metabolism	0.0384	Methane metabolism	0.0057
		Nitrogen metabolism	0.0392	Alanine, aspartate and glutamate metabolism	0.0057
		Phosphatidylinositol signaling system	0.0429	Lysine biosynthesis	0.0213
				Nitrogen metabolism	0.0255
				Citrate cycle (TCA cycle)	0.0338
				Vitamin B6 metabolism	0.0385
				Inositol phosphate metabolism	0.0390
				Monobactam biosynthesis	0.0392
				Tryptophan metabolism	0.0464

293

294 **Fig 5. Comparing differentially expressed genes (DEGs) of *gpa2* and *ras2*.** A) Venn diagram  
 295 of subsets of DEGs, for *gpa2* vs. wildtype and *ras2* vs. wildtype, after glucose addition to 2%.  
 296 Upper semicircle shows up-regulated DEGs and lower semicircle shows down-regulated DEGs.  
 297 Numbers in the overlapping region are shared DEGs regulated in the same direction. Numbers in  
 298 parenthesis are shared DEGs regulated in the opposite direction, and are placed in the area  
 299 corresponding to the direction of regulation. DEGs used for ORA analysis that are B) shared and  
 300 change in the same direction; C) unique to *ras2*; D) unique to *gpa2*. Listed are all pathways and  
 301 their functional categories with adjusted p-value <0.05.

302

303 *Metabolomics Analysis.* To better understand the relationship of large and small G  
 304 proteins, we next conducted untargeted metabolomics on the corresponding mutants after



305 glucose addition. Again, we used MetaboAnalystR for pathway enrichment analysis. In  
306 agreement with our transcriptomics data, we found that *gpa2* and *ras2* affected several common  
307 pathways related to carbohydrate and amino acid metabolism; however, *ras2* impacted a wider  
308 variety of amino acid species (Tables 3, 4, S7 and S8). Based on the Venn diagram and ORA  
309 analysis, *gpa2* and *ras2* had a large number of shared SPMs that changed in the same  
310 direction, most of which were related to carbohydrate metabolism (Fig 6 and S10 Table). In  
311 summary, two minutes after sugar addition the *gpa2* and *ras2* strains exhibited a similar  
312 metabolic profile (Fig 6). However, after ten minutes, *gpa2* and *ras2* exhibited a different  
313 transcriptional profile (Fig 5): while *gpa2* mainly affected transcripts related to carbohydrates  
314 and lipids, *ras2* impacted transcripts related to all major categories of metabolic processes. By  
315 any measure, the *ras1* mutant yielded no significant differences, at least under the experimental  
316 conditions used in this analysis.

317

318 **Fig 6. Comparing significantly perturbed metabolites (SPMs) of *gpa2* and *ras2*.** A) Venn  
319 diagram of subsets of SPMs, for *gpa2* and *ras2* vs. wildtype, after glucose addition. Upper  
320 semicircle shows up-regulated SPMs and lower semicircle shows down-regulated SPMs.  
321 Numbers in the overlapping region are shared SPMs regulated in the same direction. Numbers in  
322 parenthesis are shared SPMs regulated in the opposite direction, and are placed in the area  
323 corresponding to the direction of regulation. SPMs used for ORA analysis that are B) shared and  
324 change in the same direction. Listed are all pathways and their functional categories with adjusted  
325 p-value <0.05.

326

327 *Integration analysis.* We then conducted integration analysis using the joint pathway  
328 analysis module in MetaboAnalystR. By this method we found that Ras2, like Gpa2, regulated  
329 pathways related to carbohydrate, purine and certain amino acids metabolism (Tables 3, 4, S7  
330 and S8). The extent of overlap was particularly evident through integration of the metabolomics

331 and transcriptomics analysis. The *ras2* strain was unique in regulating additional amino acids,  
332 as well as lipid and vitamin metabolism (Tables 4 and S8). The *gpa2* strain was unique in  
333 regulating oxidative phosphorylation and  $\beta$ -alanine metabolism (Tables 3 and S7). The results  
334 obtained using MetaboAnalystR were reflected in the high confidence annotations obtained  
335 using our in-house library.

336 To visualize the functional relationship of Ras2 and Gpa2, we projected the inputs of our  
337 integration analysis onto the pertinent yeast metabolic pathways in KEGG. From this  
338 visualization, it is evident that the effects of Gpa2 are centered on carbohydrate and energy  
339 metabolism, which is shared by Ras2 (Figs 7A and S4). In addition, Ras2 also affects a  
340 substantial number of different metabolic species (Figs 7B and S5).

341  
342 **Fig 7. KEGG pathways regulated by GPA2 or RAS2.** The relevant part of a specific KEGG  
343 pathway is shown with genes displayed as rectangles and metabolites displayed as circles. KEGG  
344 compound name for each metabolite is labeled beside the circle. Standard gene names are  
345 labeled inside the rectangle. For enzyme complexes, the gene name for the major component is  
346 shown followed with an ellipsis. The directions of irreversible enzymatic reactions are shown by  
347 the arrows. Reversible reactions are connected by straight lines. DEGs and SPMs are highlighted  
348 in orange (*gpa2*) and purple (*ras2*). Shared DEGs and SPMs are colored half orange and half  
349 purple. A) both *gpa2* and *ras2* affected components in glycolysis / gluconeogenesis (functional  
350 category: carbohydrate); B) as compared with *gpa2*, *ras2* affected more components in glycine,  
351 serine and threonine metabolism (functional category: amino acid).

352  
353 To summarize, we observed three major differences when comparing *gpr1* vs. *snf3 rgt2*  
354 and *gpa2* vs. *ras2*. First, the large and small G proteins (Gpa2 and Ras2) had concordant  
355 effects on genes and metabolites while the effects of the GPCR (Gpr1) and the transceptors  
356 (Snf3 and Rgt2) were largely opposing. Second, Ras2 had considerable effects on carbohydrate

357 metabolism while Snf3 and Rgt2 had little effect on these processes. Third, Ras2, like Snf3 and  
358 Rgt2, affected non-carbohydrate-related pathways. However, Ras2 affected far fewer genes  
359 and metabolites, as compared to Snf3 and Rgt2. These findings highlight the functional  
360 interrelationship of the two receptor systems as well as that of the large and small G proteins.

361

### 362 **Ras2 integrates signals from Gpr1 and Snf3/Rgt2.**

363 Above we show that Gpr1 is dedicated to carbohydrate metabolism while Snf3 and Rgt2  
364 primarily control the metabolism of non-carbohydrate species. The downstream G proteins,  
365 Gpa2 and Ras2, have concordant effects on carbohydrate metabolism. However, Ras2 affects  
366 additional major species that are also affected by Snf3 and Rgt2. Based on these results, we  
367 postulated that Snf3 and Rgt2 signal through Ras2. Just as Ras2 acts in synchrony with Gpr1  
368 and Gpa2 to regulate carbohydrate metabolism, we considered if Ras2 also works together with  
369 Snf3 and Rgt2 to regulate non-carbohydrate species. Upon examination of the integration  
370 analysis presented above, we determined that processes regulated by both Ras2 and Gpa2 are  
371 primarily related to carbohydrates (7 pathways shared), and to a lesser extent amino acids (3  
372 pathways shared), as well as purine metabolism (Tables 3, 4, S7 and S8). In comparison,  
373 processes regulated by both Ras2 and Snf3/Rgt2 are related to amino acids (4 pathways  
374 shared), carbohydrates (4 pathways shared), peroxisome and purines (Tables 2, 4, S3 and S8).

375 We then quantified DEGs and SPMs regulated by Ras2 as well as by Snf3 and Rgt2.  
376 These data are presented as Venn diagrams in Figs 8A and 9A (S11 and S12 Tables). In  
377 accordance with our hypothesis, ORA revealed that Ras2 and the transceptors had concordant  
378 effects on DEGs related to amino acids, energy, cofactors and vitamins (Fig 8B). While *snf3 rgt2*  
379 uniquely affected some DEGs related to purines (Fig 8C), they shared with *ras2* the ability to  
380 regulate SPMs related to the same process (Fig 9B). Furthermore, the effect of *ras2* on  
381 carbohydrates is not shared by *snf3 rgt2* (Fig 8D). We then performed qPCR to quantify the  
382 expression level of genes in wildtype, *ras2* and *snf3 rgt2* before and 10 min after glucose

383 addition. As shown in Fig 10, *ras2* and *snf3 rgt2* have concordant effects on *INO1*, which  
384 encodes an Inositol-3-phosphate synthase, and *AGX1*, the product of which catalyzes the  
385 synthesis of glycine from glyoxylate; neither enzyme is directly related to carbohydrate  
386 metabolism. Thus, multiple lines of evidence indicate that Ras2 and the transceptors share the  
387 ability to regulate non-carbohydrate metabolism.

388 As noted above, Ras2 and the transceptors had opposing effects on SPMs related to  
389 carbohydrate metabolism (Fig 9C). This unexpected effect is further supported by qPCR  
390 analysis. As shown in Fig 10, *ras2* and *snf3 rgt2* had significant yet opposing impact on *TKL2*,  
391 which encodes an enzyme in the pentose phosphate pathway, and *ALD6*, which produces an  
392 aldehyde dehydrogenase involved in pyruvate metabolism. Both enzymes participate directly in  
393 carbohydrate metabolism. Therefore, the impact of Snf3 and Rgt2 on carbohydrate metabolism  
394 is more limited and antagonistic to that of Ras2. These relationships can be viewed using the  
395 KEGG Metabolic Pathways Maps (S2-S5 Figs). Thus, Gpr1 and Ras2 regulate carbohydrate  
396 metabolism while Snf3/Rgt2 and Ras2 regulate non-carbohydrate metabolism. We conclude  
397 that Ras2 coordinates and integrates signaling by both receptor systems. By integrating  
398 transcriptomic and metabolomic measurements, we have taken a major step by identifying new  
399 and unexpected functions of Ras2 in the transceptor signaling pathway.

400

401 **Fig 8. Comparing differentially expressed genes (DEGs) of *snf3 rgt2* and *ras2*.** A) Venn  
402 diagram of subsets of DEGs, for *snf3 rgt2* vs. wildtype and *ras2* vs. wildtype, after glucose addition  
403 to 2%. Upper semicircle shows up-regulated DEGs and lower semicircle shows down-regulated  
404 DEGs. Numbers in the overlapping region are shared DEGs regulated in the same direction.  
405 Numbers in parenthesis are shared DEGs regulated in the opposite direction, and are placed in  
406 the area corresponding to the direction of regulation. DEGs used for ORA analysis that are B)  
407 shared and change in the same direction; C) unique to *snf3 rgt2*; D) unique to *ras2*. Listed are all  
408 pathways and their functional categories with adjusted p-value <0.05.

409

410 **Fig 9. Comparing significantly perturbed metabolites (SPMs) of *snf3 rgt2* and *ras2*.** A) Venn  
411 diagram of subsets of SPMs, for *snf3 rgt2* vs. wildtype and *ras2* vs. wildtype, after glucose  
412 addition. Upper semicircle shows up-regulated SPMs and lower semicircle shows down-regulated  
413 SPMs. Numbers in parenthesis are shared SPMs regulated in the opposite direction, and are  
414 placed in the area corresponding to the direction of regulation. Numbers in parenthesis are shared  
415 SPMs regulated in the opposite direction, and are placed in the area corresponding to the direction  
416 of regulation. SPMs used for ORA analysis that are B) shared and change in the same direction;  
417 C) shared and change in the opposite direction. Listed are all pathways and their functional  
418 categories with adjusted p-value <0.05.

419

420 **Fig 10. qPCR analysis.** Bar plots of qPCR data for *INO1*, *AGX1*, *TKL2*, and *ALD6* for *ras2*  
421 (purple) and *snf3 rgt2* (blue). X-axis shows target genes; Y-axis shows log<sub>2</sub> fold induction relative  
422 to wildtype. Error bars represent standard error of mean and significance marks are as follows:  
423 p<0.01(\*\*), p<0.05(\*) as determined via Mann-Whitney U test and adjusted for multiple  
424 comparisons with the Benjamini-Hochberg procedure (see Methods).

425

## 426 **DISCUSSION**

427 Here we have identified several new and important functions for the glucose sensing  
428 apparatus in yeast, comprised of a G protein coupled receptor and a transceptor dimer. Through  
429 a systematic analysis of individual gene deletion mutants, we showed how each system  
430 contributes - in both shared and unique ways - to transcription and metabolism. In addition, our  
431 integration analysis allowed us to confirm and consolidate changes seen at the metabolic or  
432 transcriptional level. Whereas the G protein-coupled receptor directs early events in glucose  
433 utilization, the transceptors regulate subsequent processes and downstream products of  
434 glucose metabolism. While the effects of Ras2 align with those of the G protein coupled

435 receptor, they also align with those of the transceptors. Based on these results, we conclude  
436 that Ras2 integrates responses from both receptor systems.

437 Our approach is distinct from that of prior work on signaling by GPCRs and other cell  
438 surface receptors. First, protein components of cell signaling pathways have traditionally been  
439 characterized one at a time, often using different readouts for different genes or proteins. Such  
440 a piecemeal approach has hindered a comprehensive understanding of the encoded signaling  
441 network. Our approach employed comprehensive genome-scale and metabolome-scale (“omic”)  
442 measures to quantify differences between mutants lacking individual genes and gene products.  
443 Second, our approach was to compare gene deletion mutants in a single-celled organism, one  
444 where it is possible to determine functional consequences in the same genetic and epigenetic  
445 background, and under identical environmental conditions. By working with yeast we circumvent  
446 challenges associated with more complex biological systems, where the structure or topology of  
447 the systems is not fully known, the inputs are not static but dynamic (and change over many  
448 time scales); such interactions are more likely to be nonlinear and to occur simultaneously at  
449 many levels of the biological hierarchy, from molecules to cells to tissues to organs and even to  
450 other organisms.

451 As part of our analysis we compared the function of the individual transceptors, Snf3 and  
452 Rgt2, as well as two small G proteins, Ras1 and Ras2. This was done in an effort to determine  
453 how these paralogous proteins each contribute to glucose signaling, and with the expectation  
454 that such analysis could provide insights into the evolutionary forces that have preserved these  
455 gene duplications. Paralogs, or duplicated genes, are especially prevalent in processes related  
456 to glucose sensing and utilization in yeast. Apart from the transceptors and Ras proteins, at  
457 least four other components of the glucose-sensing pathway (Fig 1) and 8 (out of 12) enzymes  
458 responsible for glycolysis [71], are comprised of paralogous gene products. In comparison only  
459 8% of chemical reactions in yeast are executed by paralogs. Systematic deletion of the  
460 glycolytic enzymes revealed no defect with respect to gene expression (by microarray), the

461 formation of glycolytic products, or growth rate in a variety of conditions [72]. In keeping with this  
462 pattern, our transcriptomics (by RNAseq) and metabolomics analysis (by mass spectrometry)  
463 showed that Snf3 and Rgt2 are functionally redundant; that is, deletion of both genes was  
464 needed to detect any changes in the thousands of chemical entities measured here (see Data  
465 Availability Statement). Of course it is possible that differences in fitness exist but may only be  
466 evident under very specific, non-laboratory, growth conditions [71, 73-76].

467 In the context of previous analysis of gene paralogs, we consider the most significant  
468 outcome of our analysis to be that Ras2 (but not Ras1) is required for glucose signaling, and  
469 that Ras2 is functionally linked to both receptor systems. Whereas the two receptor systems  
470 have distinct roles in signaling, Ras2 appears to integrate the two receptor pathways. Ras2, like  
471 Gpr1, directly regulates carbohydrate metabolism. Ras2, like Snf3 and Rgt2, also regulates  
472 subsequent processes related to amino acid and nitrogen metabolism. Left unresolved is the  
473 role of its paralog Ras1. One possibility is that Ras1 is primarily involved in other aspects of  
474 nutrient sensing, as demonstrated for the nitrogen-sensing pathway leading to autophagy [77].

475 In contrast to Ras2 and Ras1, either Snf3 or Rgt2 can sustain the glucose response.  
476 This begs the question, why have both paralogs been retained throughout the course of  
477 evolution? Most discussions of gene paralogs have focused on their potential contributions to  
478 genetic robustness and phenotypic plasticity [78]. Robustness refers to a number of different  
479 mechanisms that stabilize phenotype against genetic or environmental perturbations. An  
480 extreme example of robustness is where one of the genes is inactivated and the remaining copy  
481 provides enough of the original function to compensate for the loss and ensure survival. In  
482 support of this model, several studies in yeast have found that about a third of paralogous gene  
483 pairs exhibit negative epistasis [76, 79-81], meaning that deleting both copies produces a  
484 significantly larger defect than that of the individual deletions. Robustness could be important  
485 when the activity of a duplicated gene product is temporarily disabled in response to changing  
486 environmental circumstances, for example through substrate inhibition or feedback

487 phosphorylation. In that case the remaining paralog might compensate for the loss of its sibling  
488 by modifying its function through transcriptional reprogramming [82, 83], changes in protein  
489 stability and abundance [84, 85], or redistribution within the cell [78, 86, 87]. In this way, the  
490 overall system may exhibit robustness even while the underlying components exhibit functional  
491 plasticity.

492 Finally, our approach in yeast could guide investigations of functional redundancies in  
493 other signaling systems and in other organisms. For example in humans there are three  
494 subtypes of  $G\alpha_i$ , which assemble with four (out of five) subtypes of  $G\beta$  and 12 subtypes of  $G\gamma$ .  
495 Investigators have struggled to find any functional differences among various  $G\beta\gamma$  subunit  
496 combinations. Another example is the three isoforms of RAS in humans. These proteins were  
497 long thought to be functionally interchangeable, since all three share substantial sequence  
498 identity in domains responsible for nucleotide binding, GTPase activity, and most effector  
499 interactions. However, more recent investigations have shown that HRAS, NRAS and KRAS,  
500 when mutated, are each associated with a distinct group of cancer types [88]. An unresolved  
501 question is the physiological consequences of these differences with respect to metabolic  
502 programming. Moving forward, we believe that the comprehensive, multi-faceted approach  
503 taken here could help to provide mechanistic insights to differences among various G proteins in  
504 humans.

505

## 506 **METHODS**

### 507 **Yeast strains**

508 The prototrophic (wildtype) strain used throughout was constructed from BY4741 (MATa  
509 *his3 $\Delta$ 1 leu2 $\Delta$ 0 met15 $\Delta$ 0 ura3 $\Delta$ 0*). *HIS3*, *LEU2*, *MET15* and *URA3* were integrated at the  
510 endogenous loci with sequence amplified by PCR from S288C strain DNA. All single mutants  
511 (*gpr1*, *gpa2*, *ras1*, *ras2*, *snf3*, *rgt2*) were constructed by transforming the wildtype strain with



512 corresponding sequence from the Yeast Knock-Out collection that replaces the target gene with  
513 KanMX4 [89]. The *snf3 rgt2* double mutant was constructed by switching the mating type of *snf3*  
514 from MAT $\alpha$  to MAT $\alpha$ , with HO expressed from a plasmid, and then mating to an isogenic *rgt2*  
515 strain. The diploid was then sporulated and spore products with the *snf3 rgt2* double knock-out  
516 were confirmed with PCR.

517 Cells maintained at 30 °C in Synthetic Complete (SC) (2% glucose) medium were  
518 centrifuged and washed twice and then resuspended into 10 mL SC (0.05% glucose) and  
519 cultivated for 1 hour. For high and low glucose treatment, 245  $\mu$ L of 65.5% or 0.05% glucose  
520 was added to 10 mL cell culture respectively, each for exactly 2 minutes (metabolomics) or 10  
521 minutes (transcriptomics). Subsequent analysis was performed as described previously [13],  
522 and as summarized below.

#### 523 **Sample preparation for RNA-seq**

524 500  $\mu$ L of cell culture was centrifuged at 1000 x g for 1 minute at 4 °C; the resulting cell  
525 pellet was flash frozen by liquid nitrogen. Cells stored at -80 °C were resuspended with 600  $\mu$ L  
526 buffer RLT 1% (v/v) 2-mercaptoethanol from the QIAGEN RNeasy Mini Kit (Cat No.: 74106),  
527 transferred to 2 mL OMNI prefilled ceramic bead tubes (SKU: 19-632), loaded onto an OMNI  
528 Bead Mill Homogenizer (SKU:19-040E) and agitated three times at 5 m/s for 1 minute at 4 °C  
529 while cooled on ice for 3 minutes between each cycle. The resulting lysate was clarified by  
530 centrifugation at 11,000 xg and used for total RNA extraction with QIAGEN RNeasy Mini Kit  
531 (Cat No.: 74106) with on-column DNase digestion. Extracted total RNA for each sample was  
532 evaluated for purity and quantified with the Qubit RNA HS Assay kit (Cat No.: Q32855) and an  
533 Invitrogen Qubit 2.0 Fluorometer (Cat No.: Q32866), each according to manufacturer's  
534 instructions.

535 RNA libraries were prepared with Kapa stranded mRNA-seq kits, with KAPA mRNA  
536 Capture Beads (KAPA code: KK8421; Roche Cat No.: 07962207001) through the UNC High  
537 Throughput Sequencing Facility. All procedures were according to manufacturer's instructions.

## 538 **RNA Sequence analysis**

539           Quality of raw sequence was checked with the FASTQC algorithm  
540 (http://www.bioinformatics.babraham.ac.uk/projects/fastqc/). Sequence alignment to genome  
541 indices, generated based on *Saccharomyces cerevisiae* data downloaded from Ensembl.org,  
542 was performed with the STAR algorithm [90]. Quantification on the transcriptome level was  
543 performed with the SALMON algorithm [91]. Differences in transcript abundance were  
544 determined using a negative binomial generalized linear model in DESeq2 package in R [92,  
545 93]. Differentially Expressed Genes (DEGs) were defined as having adjusted p-value <0.05,  
546 absolute log2 fold-change >1 and baseMean >100. A series of baseMean thresholds have been  
547 tested, including 0, 50 and 100. The conclusion remains unchanged. Therefore, the most  
548 stringent threshold (baseMean>100, which filters out >20% of genes) was chosen for data  
549 analysis.

550           PCA analysis was performed using the internal PCA function of DESeq2 package with  
551 variance stabilizing transformation (vst) normalized data.

## 552 **Transcriptomics pathway enrichment analysis and over-representation analysis**

553           Pathway enrichment analysis for transcriptomics data was performed with ClusterProfiler  
554 package in R [63]; Log2 fold-change for each comparison (mutantH vs. wtH) was extracted from  
555 corresponding DESeq2 analysis. GSEA analysis was then performed with gseKEGG function,  
556 with organism set to 'sce' (*Saccharomyces cerevisiae*), permutation number set to 1000,  
557 minimal and maximal size for each analyzed geneset as 3 and 200, p-value cutoff set to 0.05, p-  
558 value adjustment method set to 'BH' (Benjamini-Hochberg).

559           Over-representation analysis for the corresponding subsection of the Venn diagram was  
560 performed with the enrichKEGG function in ClusterProfiler package, with organism set to 'sce'  
561 (*Saccharomyces cerevisiae*), minimal and maximal size for each analyzed geneset as 3 and  
562 200, p-value cutoff set to 0.05, p-value adjustment method set to 'BH' (Benjamini-Hochberg).

## 563 **Sample preparation for metabolomics**

564 3 mL of cell culture was mixed with 45 mL cold pure methanol on dry ice and after 5  
565 minutes centrifuged in a precooled rotor (-80 °C). Cell pellets were stored at -80 °C and  
566 resuspended with extraction reagent (8:2 methanol-water solution) to  $3 \times 10^8$  cell/mL, transferred  
567 to 2 mL ceramic bead MagNalyser tubes and subjected to homogenization with Bead Ruptor  
568 Elite Bead Mill Homogenizer (OMNI International) at 6.0 m/s for 40 seconds in 2 cycles at room  
569 temperature. This homogenization step was repeated twice. After centrifugation at 16,000 xg for  
570 10 minutes at 4 °C, 500  $\mu$ L of the supernatant was transferred into low-bind 1.7 mL microfuge  
571 tubes. Total pools were made by combining an additional 65  $\mu$ L of the supernatant from each  
572 sample and then aliquoting this mixture into low-bind 1.7 mL tubes at a volume of 500  $\mu$ L.  
573 Samples and blanks were dried using a speedvac vacuum concentrator overnight. Following  
574 storage at -80 °C, samples were resuspended in 100  $\mu$ L reconstitution buffer (95:5  
575 water:methanol with 500 ng/mL tryptophan d-5), vortexed at 5000 rpm for 10 minutes, and then  
576 centrifuged at room temperature at 16,000 xg for 4 minutes. Supernatant was transferred into  
577 autosampler vials for LC-MS.

#### 578 **UHPLC high-resolution Orbitrap MS metabolomics data acquisition**

579 Metabolomics data were acquired on a Vanquish UHPLC system coupled to a  
580 QExactive HF-X Hybrid Quadrupole-Orbitrap Mass Spectrometer (ThermoFisher Scientific, San  
581 Jose, CA), as described previously [94]. Our UPLC–MS reversed phase platform was  
582 established based on published methods [95, 96]. Metabolites were separated using an HSS T3  
583 C18 column (2.1  $\times$  100 mm, 1.7  $\mu$ m, Waters Corporation) at 50 °C with binary mobile phase of  
584 water (A) and methanol (B), each containing 0.1% formic acid (v/v). The UHPLC linear gradient  
585 started from 2% B, and increased to 100% B in 16 minutes, then held for 4 minutes, with the  
586 flow rate at 400  $\mu$ L/minute. The untargeted data were acquired in positive mode from 70 to 1050  
587 m/z using the data-dependent acquisition mode.

#### 588 **Metabolomics data normalization and filtration**

589 Progenesis QI (version 2.1, Waters Corporation) was used for peak picking, alignment,  
590 and normalization as described previously [94]. Samples were randomized and run within two  
591 batches with blanks and pools interspersed at a rate of 10%. Starting from the un-normalized  
592 data for each of the batch runs, the data were filtered so as to only include signals with an  
593 average intensity fold change of 3.0 or greater in the total pools compared to the blanks.  
594 Individual samples (including pools, blanks, and study samples) were then normalized to a  
595 reference sample that was selected by Progenesis from the total pools via a function named  
596 “normalize to all”. Signals were then excluded that were significantly different between pools of  
597 batch 1 and pools of batch 2 based on an ANOVA comparison calculated in Progenesis ( $q$   
598  $<0.05$ ). After normalization and filtration, 2397 signals passed the QC procedures and were  
599 used for further analysis.

600 The filtered and normalized data were mean-centered and Pareto scaled prior to  
601 conducting the unsupervised principal component analysis using the ropls R package

#### 602 **In-house compound identification and annotation**

603 Peaks were identified or annotated by Progenesis QI through matching to an in-house  
604 experimental standards library generated by acquiring data for approximately 1000 compounds  
605 under conditions identical to study samples, as well as to public databases (including HMDB,  
606 METLIN and NIST), as described previously [94]. Identifications and annotations were assigned  
607 using available data for retention time (RT), exact mass (MS), MS/MS fragmentation pattern,  
608 and isotopic ion pattern. The identification or annotation of each signal is provided in Supporting  
609 Information. Signals/metabolites that matched to the in-house experimental standards library by  
610 (a) RT, MS, and MS/MS are labeled as OL1, or (b) by RT and MS are labeled OL2a. An OL2b  
611 label was provided for signals that match by MS and MS/MS to the in-house library that were  
612 outside the retention time tolerance ( $\pm 0.5$  min) for the standards run under identical conditions.  
613 Signals matched to public databases are labeled as PDa (MS and experimental MS/MS), PDb

614 (MS and theoretical MS/MS), PDc (MS and isotopic similarity or adducts), and PDd (MS only)  
615 are also provided (Supporting Information).

## 616 **Compound annotation, metabolic pathway enrichment analysis and over-representation** 617 **analysis**

618 Compound annotation and pathway enrichment analysis for metabolomics was  
619 performed with the MetaboAnalystR 3.0 package in R [69, 70]  
620 (<https://www.metaboanalyst.ca/docs/RTutorial.xhtml>). For compound annotations, molecular  
621 weight tolerance (ppm) was set to 3.0, analytical mode was set to positive and retention time  
622 was included. Pathway enrichment analysis was performed with 'integ' module (using both  
623 Mummichog v2.0 and GSEA) with the yeast KEGG database. The p-value threshold for  
624 Mummichog was set at 0.05.

625 Normalized peak data from Progenesis Q1 were used as input for MetaboAnalystR. The  
626 interaction term estimated how the response amplitude of each mutant is different from wildtype,  
627 that is  $(\text{mutantH}-\text{mutantL})-(\text{wtH}-\text{wtL})$ . The modeled p-value and t score for the interaction term  
628 associated with each peak were then used as inputs for pathway enrichment analysis.  
629 Significantly perturbed metabolites (SPMs) were defined as annotations that have adjusted p-  
630 value  $<0.05$  (FDR) from the output of MetaboAnalystR. Significantly perturbed pathways were  
631 defined as having combined p-value  $<0.05$  (Mummichog and GSEA).

632 Over-representation analysis for the corresponding subsection of the Venn diagram was  
633 performed with the Enrichment Analysis module in MetaboAnalystR, with KEGG ID for each  
634 metabolite as the input. FDR adjusted p-value  $<0.05$  was the threshold for over-represented  
635 pathways.

## 636 **Integration of transcriptomics and metabolomics data**

637 Integration analysis was performed with the 'joint pathway analysis' module of  
638 MetaboAnalystR (<https://www.metaboanalyst.ca/docs/RTutorial.xhtml>). Gene input together with  
639 log<sub>2</sub> fold-change was generated based on the corresponding DESeq2 analysis, with the

640 threshold set as adjusted p-value <0.05, absolute log2 fold-change >1 and baseMean >100  
641 (DEGs); metabolite input together with log2 fold-change was generated based on  
642 MetaboAnalystR analysis, with the threshold set as adjusted p-value <0.05 (SPMs). Integration  
643 analysis was performed on 'all pathways', which includes both metabolic pathways as well as  
644 gene-only pathways. Enrichment analysis was performed using 'Hypergeometric test'. Topology  
645 measure was set to 'Degree Centrality'. Integration method was set to 'combine queries', which  
646 is a tight integration method with genes and metabolites pooled into a single query and used to  
647 perform enrichment analysis within their "pooled universe". Significantly enriched pathways  
648 were defined as having FDR adjusted p-value <0.05.

#### 649 **Yeast RNA extraction, DNase treatment, and reverse transcription for qPCR**

650 RNA was extracted from cells using hot acid phenol. TES solution (10 mM Tris-HCl, pH  
651 7.5; 10 mM EDTA; 0.5% SDS) was used to resuspend pellets then the resuspension was  
652 incubated for one hour at 65°C. The RNA was separated via phenol-chloroform extraction and  
653 any residual DNA was degraded with RQ1 DNase (Promega). To further purify the RNA,  
654 RNeasy mini kit (Qiagen) was used and the final RNA concentration was determined via  
655 spectrophotometry with a NanoDrop One (ThermoFisher Scientific). cDNA was produced via  
656 reverse transcription from 250 ng RNA using a High-Capacity cDNA Reverse Transcription Kit  
657 (ThermoFisher Scientific) following manufacturer's protocol.

#### 658 **qPCR**

659 qPCR primers were ordered from Integrated DNA Technologies:

660 YER100W\_FWD primer: 5' GAAGCCACGACAGGATCAAT 3'

661 YER100W\_REV primer: 5' ATCCCCCTCATCCAATTTTC 3'

662 YBR117C\_FWD: 5' GTCACATCATGCGCTCTTCTG 3'

663 YBR117C\_REV: 5' GAGTCGGAAATGGGAAAGCC 3'

664 YPL061W\_FWD: 5' GGCGCCAAGATCTTAACTGG 3'

665 YPL061W\_REV: 5' CCACCTTCAAACCTGTGCTC 3'

666 YJL153C\_FWD: 5' CATGGTTAGCCCAAACGACT 3'  
667 YJL153C\_REV: 5' CGTGGTTACGTTGCCTTTTT 3'  
668 YFL030W\_FWD: 5' TGATCCCAGGCCCCATTATC 3'  
669 YFL030W\_REV: 5' AATATGTCCCACCCCAACGT 3'

670 To perform qPCR, cDNA was diluted 50-fold and amplified with SsoAdvanced Universal  
671 SYBR Green Supermix (Bio-Rad) following manufacturer's protocols with adjustments: 45  
672 cycles were used to increase amplification and anneal/extension time was extended to 45  
673 seconds. qPCR was performed in technical triplicate for each of the six biological replicates per  
674 genotype. CFX Maestro Software (Bio-Rad) was used to determine the threshold cycle ( $C_t$ ).  $\Delta C_t$   
675 values were determined in reference to YER100W and final  $\Delta\Delta C_t$  values were calculated and  
676 normalized in reference to wildtype cells. p values were calculated on  $\Delta C_t$  values between  
677 genotypes via independent, non-parametric, one-tailed Mann-Whitney U tests with the expected  
678 change in expression as was found by RNAseq. One exception was that of *TKL2* in *snf3 rgt2* vs.  
679 wildtype comparison in which the RNAseq data did not yield a statistically significant change, in  
680 this case a two-sided Mann-Whitney U test was applied. The Benjamini-Hochberg Procedure  
681 was used to correct for multiple comparisons.

682

## 683 REFERENCES

- 684 1. Kresnowati MT, van Winden WA, Almering MJ, ten Pierick A, Ras C, Knijnenburg TA, et  
685 al. When transcriptome meets metabolome: fast cellular responses of yeast to sudden relief of  
686 glucose limitation. *Mol Syst Biol.* 2006;2:49. Epub 2006/09/14. doi: 10.1038/msb4100083.  
687 PubMed PMID: 16969341; PubMed Central PMCID: PMC1681515.
- 688 2. Castrillo JI, Zeef LA, Hoyle DC, Zhang N, Hayes A, Gardner DC, et al. Growth control of  
689 the eukaryote cell: a systems biology study in yeast. *J Biol.* 2007;6(2):4. Epub 2007/04/19. doi:  
690 10.1186/jbiol54. PubMed PMID: 17439666; PubMed Central PMCID: PMC1681515.

- 691 3. Gutteridge A, Pir P, Castrillo JI, Charles PD, Lilley KS, Oliver SG. Nutrient control of  
692 eukaryote cell growth: a systems biology study in yeast. *BMC Biol.* 2010;8:68. Epub 2010/05/26.  
693 doi: 10.1186/1741-7007-8-68. PubMed PMID: 20497545; PubMed Central PMCID:  
694 PMCPMC2895586.
- 695 4. Dikicioglu D, Karabekmez E, Rash B, Pir P, Kirdar B, Oliver SG. How yeast re-programmes  
696 its transcriptional profile in response to different nutrient impulses. *BMC Syst Biol.* 2011;5:148.  
697 Epub 2011/09/29. doi: 10.1186/1752-0509-5-148. PubMed PMID: 21943358; PubMed Central  
698 PMCID: PMCPMC3224505.
- 699 5. Yun CW, Tamaki H, Nakayama R, Yamamoto K, Kumagai H. G-protein coupled receptor  
700 from yeast *Saccharomyces cerevisiae*. *Biochem Biophys Res Commun.* 1997;240(2):287-92.
- 701 6. Yun CW, Tamaki H, Nakayama R, Yamamoto K, Kumagai H. Gpr1p, a putative G-protein  
702 coupled receptor, regulates glucose- dependent cellular cAMP level in yeast *Saccharomyces*  
703 *cerevisiae*. *Biochem Biophys Res Commun.* 1998;252(1):29-33.
- 704 7. Xue Y, Batlle M, Hirsch JP. GPR1 encodes a putative G protein-coupled receptor that  
705 associates with the Gpa2p Galpha subunit and functions in a Ras-independent pathway. *Embo J.*  
706 1998;17(7):1996-2007.
- 707 8. Colombo S, Ma P, Cauwenberg L, Winderickx J, Crauwels M, Teunissen A, et al.  
708 Involvement of distinct G-proteins, Gpa2 and Ras, in glucose- and intracellular acidification-  
709 induced cAMP signalling in the yeast *Saccharomyces cerevisiae*. *Embo J.* 1998;17(12):3326-41.
- 710 9. Kraakman L, Lemaire K, Ma P, Teunissen AW, Donaton MC, Van Dijck P, et al. A  
711 *Saccharomyces cerevisiae* G-protein coupled receptor, Gpr1, is specifically required for glucose



- 712 activation of the cAMP pathway during the transition to growth on glucose. *Mol Microbiol.*  
713 1999;32(5):1002-12.
- 714 10. Lorenz MC, Pan X, Harashima T, Cardenas ME, Xue Y, Hirsch JP, et al. The G protein-  
715 coupled receptor *gpr1* is a nutrient sensor that regulates pseudohyphal differentiation in  
716 *Saccharomyces cerevisiae*. *Genetics*. 2000;154(2):609-22.
- 717 11. Lemaire K, Van de Velde S, Van Dijck P, Thevelein JM. Glucose and sucrose act as agonist  
718 and mannose as antagonist ligands of the G protein-coupled receptor *Gpr1* in the yeast  
719 *Saccharomyces cerevisiae*. *Mol Cell*. 2004;16(2):293-9. PubMed PMID: 15494315.
- 720 12. Zeller CE, Parnell SC, Dohlman HG. The RACK1 ortholog *Asc1* functions as a G-protein  
721 beta subunit coupled to glucose responsiveness in yeast. *J Biol Chem*. 2007;282(34):25168-76.  
722 PubMed PMID: 17591772.
- 723 13. Li S, Li Y, Rushing BR, Harris SE, McRitchie SL, Jones JC, et al. Multi-omics analysis of  
724 glucose-mediated signaling by a moonlighting Gbeta protein *Asc1/RACK1*. *PLoS Genet*.  
725 2021;17(7):e1009640. Epub 2021/07/03. doi: 10.1371/journal.pgen.1009640. PubMed PMID:  
726 34214075; PubMed Central PMCID: PMC8282090 paid employee of Metabolon, a for-profit  
727 company. Metabolon provided no data, data analysis, employment or consultancy, and claims  
728 no rights to possible patents or products that may arise from the research.
- 729 14. Broek D, Toda T, Michaeli T, Levin L, Birchmeier C, Zoller M, et al. The *S. cerevisiae*  
730 *CDC25* gene product regulates the RAS/adenylate cyclase pathway. *Cell*. 1987;48(5):789-99.  
731 PubMed PMID: 3545497.
- 732 15. Munder T, Kuntzel H. Glucose-induced cAMP signaling in *Saccharomyces cerevisiae* is  
733 mediated by the *CDC25* protein. *FEBS Lett*. 1989;242(2):341-5. PubMed PMID: 2536619.

- 734 16. Crechet JB, Pouillet P, Mistou MY, Parmeggiani A, Camonis J, Boy-Marcotte E, et al.  
735 Enhancement of the GDP-GTP exchange of RAS proteins by the carboxyl-terminal domain of  
736 SCD25. *Science*. 1990;248(4957):866-8. PubMed PMID: 2188363.
- 737 17. Jones S, Vignais ML, Broach JR. The CDC25 protein of *Saccharomyces cerevisiae*  
738 promotes exchange of guanine nucleotides bound to ras. *Mol Cell Biol*. 1991;11(5):2641-6.  
739 Epub 1991/05/01. PubMed PMID: 2017169; PubMed Central PMCID: PMC360033.
- 740 18. Papasavvas S, Arkininstall S, Reid J, Payton M. Yeast alpha-mating factor receptor and G-  
741 protein-linked adenylyl cyclase inhibition requires RAS2 and GPA2 activities. *Biochem Biophys*  
742 *Res Commun*. 1992;184(3):1378-85. PubMed PMID: 1317171.
- 743 19. Boy-Marcotte E, Ikonomi P, Jacquet M. SDC25, a dispensable Ras guanine nucleotide  
744 exchange factor of *Saccharomyces cerevisiae* differs from CDC25 by its regulation. *Mol Biol Cell*.  
745 1996;7(4):529-39. PubMed PMID: 8730097; PubMed Central PMCID: PMC275907.
- 746 20. Gross A, Winograd S, Marbach I, Levitzki A. The N-terminal half of Cdc25 is essential for  
747 processing glucose signaling in *Saccharomyces cerevisiae*. *Biochemistry*. 1999;38(40):13252-62.  
748 PubMed PMID: 10529198.
- 749 21. VanderSluis B, Hess DC, Pesyna C, Krumholz EW, Syed T, Szappanos B, et al. Broad  
750 metabolic sensitivity profiling of a prototrophic yeast deletion collection. *Genome Biol*.  
751 2014;15(4):R64. Epub 2014/04/12. doi: 10.1186/gb-2014-15-4-r64. PubMed PMID: 24721214;  
752 PubMed Central PMCID: PMCPMC4053978.
- 753 22. Powers S, Kataoka T, Fasano O, Goldfarb M, Strathern J, Broach J, et al. Genes in *S*.  
754 *cerevisiae* encoding proteins with domains homologous to the mammalian ras proteins. *Cell*.  
755 1984;36(3):607-12. PubMed PMID: 6365329.

- 756 23. Toda T, Uno I, Ishikawa T, Powers S, Kataoka T, Broek D, et al. In yeast, RAS proteins are  
757 controlling elements of adenylate cyclase. *Cell*. 1985;40(1):27-36. Epub 1985/01/01. doi: 0092-  
758 8674(85)90305-8 [pii]. PubMed PMID: 2981630.
- 759 24. Uno I, Mitsuzawa H, Matsumoto K, Tanaka K, Oshima T, Ishikawa T. Reconstitution of  
760 the GTP-dependent adenylate cyclase from products of the yeast CYR1 and RAS2 genes in  
761 *Escherichia coli*. *Proc Natl Acad Sci U S A*. 1985;82(23):7855-9. Epub 1985/12/01. PubMed  
762 PMID: 2999779; PubMed Central PMCID: PMC390868.
- 763 25. Field J, Nikawa J, Broek D, MacDonald B, Rodgers L, Wilson IA, et al. Purification of a  
764 RAS-responsive adenylyl cyclase complex from *Saccharomyces cerevisiae* by use of an epitope  
765 addition method. *Mol Cell Biol*. 1988;8(5):2159-65. PubMed PMID: 2455217; PubMed Central  
766 PMCID: PMC363397.
- 767 26. Nakafuku M, Obara T, Kaibuchi K, Miyajima I, Miyajima A, Itoh H, et al. Isolation of a  
768 second yeast *Saccharomyces cerevisiae* gene (GPA2) coding for guanine nucleotide-binding  
769 regulatory protein: studies on its structure and possible functions. *Proc Natl Acad Sci U S A*.  
770 1988;85(5):1374-8.
- 771 27. Field J, Xu HP, Michaeli T, Ballester R, Sass P, Wigler M, et al. Mutations of the adenylyl  
772 cyclase gene that block RAS function in *Saccharomyces cerevisiae*. *Science*.  
773 1990;247(4941):464-7. PubMed PMID: 2405488.
- 774 28. Suzuki N, Choe HR, Nishida Y, Yamawaki-Kataoka Y, Ohnishi S, Tamaoki T, et al. Leucine-  
775 rich repeats and carboxyl terminus are required for interaction of yeast adenylate cyclase with  
776 RAS proteins. *Proc Natl Acad Sci U S A*. 1990;87(22):8711-5. PubMed PMID: 2247439; PubMed  
777 Central PMCID: PMCPMC55029.

- 778 29. Mintzer KA, Field J. Interactions between adenylyl cyclase, CAP and RAS from  
779 *Saccharomyces cerevisiae*. *Cell Signal*. 1994;6(6):681-94. PubMed PMID: 7531994.
- 780 30. Bhattacharya S, Chen L, Broach JR, Powers S. Ras membrane targeting is essential for  
781 glucose signaling but not for viability in yeast. *Proc Natl Acad Sci U S A*. 1995;92(7):2984-8.
- 782 31. Kubler E, Mosch HU, Rupp S, Lisanti MP. Gpa2p, a G-protein alpha-subunit, regulates  
783 growth and pseudohyphal development in *Saccharomyces cerevisiae* via a cAMP-dependent  
784 mechanism. *J Biol Chem*. 1997;272(33):20321-3.
- 785 32. Rolland F, De Winde JH, Lemaire K, Boles E, Thevelein JM, Winderickx J. Glucose-induced  
786 cAMP signalling in yeast requires both a G-protein coupled receptor system for extracellular  
787 glucose detection and a separable hexose kinase-dependent sensing process. *Mol Microbiol*.  
788 2000;38(2):348-58. PubMed PMID: 11069660.
- 789 33. Wang Y, Pierce M, Schnepfer L, Guldal CG, Zhang X, Tavazoie S, et al. Ras and Gpa2  
790 mediate one branch of a redundant glucose signaling pathway in yeast. *PLoS Biol*.  
791 2004;2(5):E128. doi: 10.1371/journal.pbio.0020128. PubMed PMID: 15138498; PubMed Central  
792 PMCID: PMC406390.
- 793 34. Matsumoto K, Uno I, Oshima Y, Ishikawa T. Isolation and characterization of yeast  
794 mutants deficient in adenylate cyclase and cAMP-dependent protein kinase. *Proc Natl Acad Sci*  
795 *U S A*. 1982;79(7):2355-9. PubMed PMID: 6285379; PubMed Central PMCID: PMC346192.
- 796 35. Kataoka T, Broek D, Wigler M. DNA sequence and characterization of the *S. cerevisiae*  
797 gene encoding adenylate cyclase. *Cell*. 1985;43(2 Pt 1):493-505. PubMed PMID: 2934138.

- 798 36. Casperson GF, Walker N, Bourne HR. Isolation of the gene encoding adenylate cyclase in  
799 *Saccharomyces cerevisiae*. Proc Natl Acad Sci U S A. 1985;82(15):5060-3. PubMed PMID:  
800 2991907; PubMed Central PMCID: PMC390498.
- 801 37. Harashima T, Heitman J. The Galpha protein Gpa2 controls yeast differentiation by  
802 interacting with kelch repeat proteins that mimic Gbeta subunits. Mol Cell. 2002;10(1):163-73.  
803 PubMed PMID: 12150916.
- 804 38. Toda T, Cameron S, Sass P, Zoller M, Scott JD, McMullen B, et al. Cloning and  
805 characterization of BCY1, a locus encoding a regulatory subunit of the cyclic AMP-dependent  
806 protein kinase in *Saccharomyces cerevisiae*. Mol Cell Biol. 1987;7(4):1371-7. Epub 1987/04/01.  
807 PubMed PMID: 3037314; PubMed Central PMCID: PMC365223.
- 808 39. Toda T, Cameron S, Sass P, Zoller M, Wigler M. Three different genes in *S. cerevisiae*  
809 encode the catalytic subunits of the cAMP-dependent protein kinase. Cell. 1987;50(2):277-87.  
810 Epub 1987/07/17. doi: 0092-8674(87)90223-6 [pii]. PubMed PMID: 3036373.
- 811 40. Cannon JF, Tatchell K. Characterization of *Saccharomyces cerevisiae* genes encoding  
812 subunits of cyclic AMP-dependent protein kinase. Mol Cell Biol. 1987;7(8):2653-63. PubMed  
813 PMID: 2823100; PubMed Central PMCID: PMC367881.
- 814 41. Robertson LS, Fink GR. The three yeast A kinases have specific signaling functions in  
815 pseudohyphal growth. Proc Natl Acad Sci U S A. 1998;95(23):13783-7.
- 816 42. Pan X, Heitman J. Cyclic AMP-dependent protein kinase regulates pseudohyphal  
817 differentiation in *Saccharomyces cerevisiae*. Mol Cell Biol. 1999;19(7):4874-87.

- 818 43. Robertson LS, Causton HC, Young RA, Fink GR. The yeast A kinases differentially regulate  
819 iron uptake and respiratory function. *Proc Natl Acad Sci U S A*. 2000;97(11):5984-8. doi:  
820 10.1073/pnas.100113397. PubMed PMID: 10811893; PubMed Central PMCID: PMC18545.
- 821 44. Ptacek J, Devgan G, Michaud G, Zhu H, Zhu X, Fasolo J, et al. Global analysis of protein  
822 phosphorylation in yeast. *Nature*. 2005;438(7068):679-84. Epub 2005/12/02. doi: nature04187  
823 [pii]  
824 10.1038/nature04187. PubMed PMID: 16319894.
- 825 45. Neugeborn L, Schwartzberg P, Reid R, Carlson M. Null mutations in the SNF3 gene of  
826 *Saccharomyces cerevisiae* cause a different phenotype than do previously isolated missense  
827 mutations. *Mol Cell Biol*. 1986;6(11):3569-74. PubMed PMID: 3540596; PubMed Central  
828 PMCID: PMC367116.
- 829 46. Ozcan S, Dover J, Rosenwald AG, Wolfi S, Johnston M. Two glucose transporters in  
830 *Saccharomyces cerevisiae* are glucose sensors that generate a signal for induction of gene  
831 expression. *Proc Natl Acad Sci U S A*. 1996;93(22):12428-32. PubMed PMID: 8901598; PubMed  
832 Central PMCID: PMC38008.
- 833 47. Ozcan S, Dover J, Johnston M. Glucose sensing and signaling by two glucose receptors in  
834 the yeast *Saccharomyces cerevisiae*. *EMBO J*. 1998;17(9):2566-73. doi:  
835 10.1093/emboj/17.9.2566. PubMed PMID: 9564039; PubMed Central PMCID: PMC1170598.
- 836 48. Schmidt MC, McCartney RR, Zhang X, Tillman TS, Solimeo H, Wolfi S, et al. Std1 and  
837 Mth1 proteins interact with the glucose sensors to control glucose-regulated gene expression in  
838 *Saccharomyces cerevisiae*. *Mol Cell Biol*. 1999;19(7):4561-71. PubMed PMID: 10373505;  
839 PubMed Central PMCID: PMC84254.

- 840 49. Lafuente MJ, Gancedo C, Jauniaux JC, Gancedo JM. Mth1 receives the signal given by the  
841 glucose sensors Snf3 and Rgt2 in *Saccharomyces cerevisiae*. *Mol Microbiol.* 2000;35(1):161-72.  
842 PubMed PMID: 10632886.
- 843 50. Spielewoy N, Flick K, Kalashnikova TI, Walker JR, Wittenberg C. Regulation and  
844 recognition of SCFGrr1 targets in the glucose and amino acid signaling pathways. *Mol Cell Biol.*  
845 2004;24(20):8994-9005. doi: 10.1128/MCB.24.20.8994-9005.2004. PubMed PMID: 15456873;  
846 PubMed Central PMCID: PMC517892.
- 847 51. Moriya H, Johnston M. Glucose sensing and signaling in *Saccharomyces cerevisiae*  
848 through the Rgt2 glucose sensor and casein kinase I. *Proc Natl Acad Sci U S A.*  
849 2004;101(6):1572-7. doi: 10.1073/pnas.0305901101. PubMed PMID: 14755054; PubMed  
850 Central PMCID: PMC341776.
- 851 52. Pasula S, Jouandot D, 2nd, Kim JH. Biochemical evidence for glucose-independent  
852 induction of HXT expression in *Saccharomyces cerevisiae*. *FEBS Lett.* 2007;581(17):3230-4. doi:  
853 10.1016/j.febslet.2007.06.013. PubMed PMID: 17586499; PubMed Central PMCID:  
854 PMC2040036.
- 855 53. Tomas-Cobos L, Sanz P. Active Snf1 protein kinase inhibits expression of the  
856 *Saccharomyces cerevisiae* HXT1 glucose transporter gene. *Biochem J.* 2002;368(Pt 2):657-63.  
857 doi: 10.1042/BJ20020984. PubMed PMID: 12220226; PubMed Central PMCID: PMC1223017.
- 858 54. Kim JH, Polish J, Johnston M. Specificity and regulation of DNA binding by the yeast  
859 glucose transporter gene repressor Rgt1. *Mol Cell Biol.* 2003;23(15):5208-16. PubMed PMID:  
860 12861007; PubMed Central PMCID: PMC165726.

- 861 55. Flick KM, Spielewoy N, Kalashnikova TI, Guaderrama M, Zhu Q, Chang HC, et al. Grr1-  
862 dependent inactivation of Mth1 mediates glucose-induced dissociation of Rgt1 from HXT gene  
863 promoters. *Mol Biol Cell*. 2003;14(8):3230-41. doi: 10.1091/mbc.E03-03-0135. PubMed PMID:  
864 12925759; PubMed Central PMCID: PMC181563.
- 865 56. Mosley AL, Lakshmanan J, Aryal BK, Ozcan S. Glucose-mediated phosphorylation  
866 converts the transcription factor Rgt1 from a repressor to an activator. *J Biol Chem*.  
867 2003;278(12):10322-7. doi: 10.1074/jbc.M212802200. PubMed PMID: 12527758.
- 868 57. Lakshmanan J, Mosley AL, Ozcan S. Repression of transcription by Rgt1 in the absence of  
869 glucose requires Std1 and Mth1. *Curr Genet*. 2003;44(1):19-25. doi: 10.1007/s00294-003-0423-  
870 2. PubMed PMID: 14508605.
- 871 58. Polish JA, Kim JH, Johnston M. How the Rgt1 transcription factor of *Saccharomyces*  
872 *cerevisiae* is regulated by glucose. *Genetics*. 2005;169(2):583-94. doi:  
873 10.1534/genetics.104.034512. PubMed PMID: 15489524; PubMed Central PMCID:  
874 PMC1449106.
- 875 59. Kim JH, Johnston M. Two glucose-sensing pathways converge on Rgt1 to regulate  
876 expression of glucose transporter genes in *Saccharomyces cerevisiae*. *J Biol Chem*.  
877 2006;281(36):26144-9. doi: 10.1074/jbc.M603636200. PubMed PMID: 16844691.
- 878 60. Palomino A, Herrero P, Moreno F. Tpk3 and Snf1 protein kinases regulate Rgt1  
879 association with *Saccharomyces cerevisiae* HXK2 promoter. *Nucleic Acids Res*. 2006;34(5):1427-  
880 38. doi: 10.1093/nar/gkl028. PubMed PMID: 16528100; PubMed Central PMCID: PMC1401511.
- 881 61. Jouandot D, 2nd, Roy A, Kim JH. Functional dissection of the glucose signaling pathways  
882 that regulate the yeast glucose transporter gene (HXT) repressor Rgt1. *J Cell Biochem*.



- 883 2011;112(11):3268-75. doi: 10.1002/jcb.23253. PubMed PMID: 21748783; PubMed Central  
884 PMCID: PMC3341738.
- 885 62. Roy A, Shin YJ, Cho KH, Kim JH. Mth1 regulates the interaction between the Rgt1  
886 repressor and the Ssn6-Tup1 corepressor complex by modulating PKA-dependent  
887 phosphorylation of Rgt1. *Mol Biol Cell*. 2013;24(9):1493-503. doi: 10.1091/mbc.E13-01-0047.  
888 PubMed PMID: 23468525; PubMed Central PMCID: PMC3639059.
- 889 63. Yu G, Wang LG, Han Y, He QY. clusterProfiler: an R package for comparing biological  
890 themes among gene clusters. *OMICS*. 2012;16(5):284-7. Epub 2012/03/30. doi:  
891 10.1089/omi.2011.0118. PubMed PMID: 22455463; PubMed Central PMCID: PMCPMC3339379.
- 892 64. Kanehisa M, Goto S. KEGG: kyoto encyclopedia of genes and genomes. *Nucleic Acids*  
893 *Res*. 2000;28(1):27-30. Epub 1999/12/11. doi: 10.1093/nar/28.1.27. PubMed PMID: 10592173;  
894 PubMed Central PMCID: PMCPMC102409.
- 895 65. Kanehisa M. Toward understanding the origin and evolution of cellular organisms.  
896 *Protein Sci*. 2019;28(11):1947-51. Epub 2019/08/24. doi: 10.1002/pro.3715. PubMed PMID:  
897 31441146; PubMed Central PMCID: PMCPMC6798127.
- 898 66. Kanehisa M, Furumichi M, Sato Y, Ishiguro-Watanabe M, Tanabe M. KEGG: integrating  
899 viruses and cellular organisms. *Nucleic Acids Res*. 2020. Epub 2020/10/31. doi:  
900 10.1093/nar/gkaa970. PubMed PMID: 33125081.
- 901 67. Zhang N, Cao L. Starvation signals in yeast are integrated to coordinate metabolic  
902 reprogramming and stress response to ensure longevity. *Curr Genet*. 2017;63(5):839-43. Epub  
903 2017/04/27. doi: 10.1007/s00294-017-0697-4. PubMed PMID: 28444510; PubMed Central  
904 PMCID: PMCPMC5605593.

- 905 68. Li S, Park Y, Duraisingham S, Strobel FH, Khan N, Soltow QA, et al. Predicting network  
906 activity from high throughput metabolomics. *PLoS Comput Biol.* 2013;9(7):e1003123. Epub  
907 2013/07/19. doi: 10.1371/journal.pcbi.1003123. PubMed PMID: 23861661; PubMed Central  
908 PMCID: PMC3701697.
- 909 69. Chong J, Wishart DS, Xia J. Using MetaboAnalyst 4.0 for Comprehensive and Integrative  
910 Metabolomics Data Analysis. *Curr Protoc Bioinformatics.* 2019;68(1):e86. Epub 2019/11/23.  
911 doi: 10.1002/cpbi.86. PubMed PMID: 31756036.
- 912 70. Pang Z, Chong J, Li S, Xia J. MetaboAnalystR 3.0: Toward an Optimized Workflow for  
913 Global Metabolomics. *Metabolites.* 2020;10(5). Epub 2020/05/13. doi:  
914 10.3390/metabo10050186. PubMed PMID: 32392884.
- 915 71. Bradley PH, Gibney PA, Botstein D, Troyanskaya OG, Rabinowitz JD. Minor Isozymes  
916 Tailor Yeast Metabolism to Carbon Availability. *mSystems.* 2019;4(1). Epub 2019/03/06. doi:  
917 10.1128/mSystems.00170-18. PubMed PMID: 30834327; PubMed Central PMCID:  
918 PMC6392091.
- 919 72. Solis-Escalante D, Kuijpers NG, Barrajon-Simancas N, van den Broek M, Pronk JT, Daran  
920 JM, et al. A Minimal Set of Glycolytic Genes Reveals Strong Redundancies in *Saccharomyces*  
921 *cerevisiae* Central Metabolism. *Eukaryot Cell.* 2015;14(8):804-16. Epub 2015/06/14. doi:  
922 10.1128/EC.00064-15. PubMed PMID: 26071034; PubMed Central PMCID: PMC4519752.
- 923 73. Giaever G, Chu AM, Ni L, Connelly C, Riles L, Veronneau S, et al. Functional profiling of  
924 the *Saccharomyces cerevisiae* genome. *Nature.* 2002;418(6896):387-91.

- 925 74. Papp B, Pal C, Hurst LD. Metabolic network analysis of the causes and evolution of  
926 enzyme dispensability in yeast. *Nature*. 2004;429(6992):661-4. Epub 2004/06/11. doi:  
927 10.1038/nature02636. PubMed PMID: 15190353.
- 928 75. Ihmels J, Collins SR, Schuldiner M, Krogan NJ, Weissman JS. Backup without redundancy:  
929 genetic interactions reveal the cost of duplicate gene loss. *Mol Syst Biol*. 2007;3:86. Epub  
930 2007/03/29. doi: 10.1038/msb4100127. PubMed PMID: 17389874; PubMed Central PMCID:  
931 PMCPMC1847942.
- 932 76. DeLuna A, Vetsigian K, Shores N, Hegreness M, Colon-Gonzalez M, Chao S, et al.  
933 Exposing the fitness contribution of duplicated genes. *Nat Genet*. 2008;40(5):676-81. Epub  
934 2008/04/15. doi: 10.1038/ng.123. PubMed PMID: 18408719.
- 935 77. Jin X, Starke S, Li Y, Sethupathi S, Kung G, Dodhiawala P, et al. Nitrogen Starvation-  
936 induced Phosphorylation of Ras1 Protein and Its Potential Role in Nutrient Signaling and Stress  
937 Response. *J Biol Chem*. 2016;291(31):16231-9. Epub 2016/06/05. doi:  
938 10.1074/jbc.M115.713206. PubMed PMID: 27261458; PubMed Central PMCID:  
939 PMCPMC4965571.
- 940 78. Nijhout HF, Sadre-Marandi F, Best J, Reed MC. Systems Biology of Phenotypic  
941 Robustness and Plasticity. *Integr Comp Biol*. 2017;57(2):171-84. Epub 2017/09/02. doi:  
942 10.1093/icb/icx076. PubMed PMID: 28859407.
- 943 79. Dean EJ, Davis JC, Davis RW, Petrov DA. Pervasive and persistent redundancy among  
944 duplicated genes in yeast. *PLoS Genet*. 2008;4(7):e1000113. Epub 2008/07/08. doi:  
945 10.1371/journal.pgen.1000113. PubMed PMID: 18604285; PubMed Central PMCID:  
946 PMCPMC2440806.

- 947 80. Musso G, Costanzo M, Huangfu M, Smith AM, Paw J, San Luis BJ, et al. The extensive and  
948 condition-dependent nature of epistasis among whole-genome duplicates in yeast. *Genome*  
949 *Res.* 2008;18(7):1092-9. Epub 2008/05/09. doi: 10.1101/gr.076174.108. PubMed PMID:  
950 18463300; PubMed Central PMCID: PMCPMC2493398.
- 951 81. VanderSluis B, Bellay J, Musso G, Costanzo M, Papp B, Vizeacoumar FJ, et al. Genetic  
952 interactions reveal the evolutionary trajectories of duplicate genes. *Mol Syst Biol.* 2010;6:429.  
953 Epub 2010/11/18. doi: 10.1038/msb.2010.82. PubMed PMID: 21081923; PubMed Central  
954 PMCID: PMCPMC3010121.
- 955 82. Gu X, Zhang Z, Huang W. Rapid evolution of expression and regulatory divergences after  
956 yeast gene duplication. *Proc Natl Acad Sci U S A.* 2005;102(3):707-12. Epub 2005/01/14. doi:  
957 10.1073/pnas.0409186102. PubMed PMID: 15647348; PubMed Central PMCID:  
958 PMCPMC545572.
- 959 83. Kafri R, Bar-Even A, Pilpel Y. Transcription control reprogramming in genetic backup  
960 circuits. *Nat Genet.* 2005;37(3):295-9. Epub 2005/02/22. doi: 10.1038/ng1523. PubMed PMID:  
961 15723064.
- 962 84. DeLuna A, Springer M, Kirschner MW, Kishony R. Need-based up-regulation of protein  
963 levels in response to deletion of their duplicate genes. *PLoS Biol.* 2010;8(3):e1000347. Epub  
964 2010/04/03. doi: 10.1371/journal.pbio.1000347. PubMed PMID: 20361019; PubMed Central  
965 PMCID: PMCPMC2846854.
- 966 85. van der Lee R, Lang B, Kruse K, Gsponer J, Sanchez de Groot N, Huynen MA, et al.  
967 Intrinsically disordered segments affect protein half-life in the cell and during evolution. *Cell*

- 968 Rep. 2014;8(6):1832-44. Epub 2014/09/16. doi: 10.1016/j.celrep.2014.07.055. PubMed PMID:  
969 25220455; PubMed Central PMCID: PMC4358326.
- 970 86. Stelling J, Sauer U, Szallasi Z, Doyle FJ, 3rd, Doyle J. Robustness of cellular functions. Cell.  
971 2004;118(6):675-85. Epub 2004/09/17. doi: 10.1016/j.cell.2004.09.008. PubMed PMID:  
972 15369668.
- 973 87. Kitano H. Biological robustness. Nat Rev Genet. 2004;5(11):826-37. Epub 2004/11/03.  
974 doi: 10.1038/nrg1471. PubMed PMID: 15520792.
- 975 88. Zhou B, Der CJ, Cox AD. The role of wild type RAS isoforms in cancer. Semin Cell Dev  
976 Biol. 2016;58:60-9. Epub 2016/07/17. doi: 10.1016/j.semcd.2016.07.012. PubMed PMID:  
977 27422332; PubMed Central PMCID: PMC5028303.
- 978 89. Brachmann CB, Davies A, Cost GJ, Caputo E, Li J, Hieter P, et al. Designer deletion strains  
979 derived from *Saccharomyces cerevisiae* S288C: a useful set of strains and plasmids for PCR-  
980 mediated gene disruption and other applications. Yeast. 1998;14(2):115-32.
- 981 90. Dobin A, Davis CA, Schlesinger F, Drenkow J, Zaleski C, Jha S, et al. STAR: ultrafast  
982 universal RNA-seq aligner. Bioinformatics. 2013;29(1):15-21. Epub 2012/10/30. doi:  
983 10.1093/bioinformatics/bts635. PubMed PMID: 23104886; PubMed Central PMCID:  
984 PMC3530905.
- 985 91. Patro R, Duggal G, Love MI, Irizarry RA, Kingsford C. Salmon provides fast and bias-aware  
986 quantification of transcript expression. Nat Methods. 2017;14(4):417-9. Epub 2017/03/07. doi:  
987 10.1038/nmeth.4197. PubMed PMID: 28263959; PubMed Central PMCID: PMC5600148.
- 988 92. Love MI, Huber W, Anders S. Moderated estimation of fold change and dispersion for  
989 RNA-seq data with DESeq2. Genome Biol. 2014;15(12):550. Epub 2014/12/18. doi:

- 990 10.1186/s13059-014-0550-8. PubMed PMID: 25516281; PubMed Central PMCID:  
991 PMCPMC4302049.
- 992 93. Love MI, Anders S, Kim V, Huber W. RNA-Seq workflow: gene-level exploratory analysis  
993 and differential expression. *F1000Res*. 2015;4:1070. Epub 2015/12/18. doi:  
994 10.12688/f1000research.7035.1. PubMed PMID: 26674615; PubMed Central PMCID:  
995 PMCPMC4670015.
- 996 94. Li YY, Douillet C, Huang M, Beck R, Sumner SJ, Styblo M. Exposure to inorganic arsenic  
997 and its methylated metabolites alters metabolomics profiles in INS-1 832/13 insulinoma cells  
998 and isolated pancreatic islets. *Arch Toxicol*. 2020;94(6):1955-72. Epub 2020/04/12. doi:  
999 10.1007/s00204-020-02729-y. PubMed PMID: 32277266.
- 1000 95. Zelena E, Dunn WB, Broadhurst D, Francis-McIntyre S, Carroll KM, Begley P, et al.  
1001 Development of a robust and repeatable UPLC-MS method for the long-term metabolomic  
1002 study of human serum. *Anal Chem*. 2009;81(4):1357-64. Epub 2009/01/28. doi:  
1003 10.1021/ac8019366. PubMed PMID: 19170513.
- 1004 96. Dunn WB, Broadhurst D, Begley P, Zelena E, Francis-McIntyre S, Anderson N, et al.  
1005 Procedures for large-scale metabolic profiling of serum and plasma using gas chromatography  
1006 and liquid chromatography coupled to mass spectrometry. *Nat Protoc*. 2011;6(7):1060-83. Epub  
1007 2011/07/02. doi: 10.1038/nprot.2011.335. PubMed PMID: 21720319.
- 1008  
1009

1010 **SUPPORTING INFORMATION**

1011

1012 **S1 Fig. PCA plots.** For A) transcriptomics and B) metabolomics, X-axis shows PC1 with the  
1013 percentage of explained variance and Y-axis shows PC2 with the percentage of explained  
1014 variance. Data are scaled as detailed in Methods. Wildtype (black), *gpr1* (red), *gpa2* (orange),  
1015 *snf3 rgt2* (blue), *ras1* (green), *ras2* (purple). Low glucose (L, 0.05% glucose)-triangles, high  
1016 glucose (H, 2% glucose)-circles.

1017

1018 **S2 Fig. Overview of DEGs and SPMs regulated by *GPR1* projected on KEGG Metabolic**  
1019 **Pathway.** The map is color coded to delineate carbohydrate metabolism (blue), glycan  
1020 biosynthesis and metabolism (cyan), amino acid metabolism (yellow), nucleotide metabolism  
1021 (red), lipid metabolism (teal), metabolism of cofactors and vitamins (pink). Highlighted are the  
1022 DEGs (black lines) and SPMs (black dots) for *gpr1* integration analysis and gray boxes are used  
1023 to delineate clusters associated with a specific pathway.

1024

1025 **S3 Fig. Overview of DEGs and SPMs regulated by *SNF3* and *RGT2* projected on KEGG**  
1026 **Metabolic Pathway.** The map is color coded as in S2 Fig. Highlighted are the DEGs (black lines)  
1027 and SPMs (black dots) for *snf3 rgt2* integration analysis and gray boxes are used to delineate  
1028 clusters associated with a specific pathway.

1029

1030 **S4 Fig. Overview of DEGs and SPMs regulated by *GPA2* projected on KEGG Metabolic**  
1031 **Pathway.** The map is color coded as in S2 Fig. Highlighted are the DEGs (black lines) and SPMs  
1032 (black dots) for *gpa2* integration analysis and gray boxes are used to delineate clusters associated  
1033 with a specific pathway.

1034

1035 **S5 Fig. Overview of DEGs and SPMs regulated by RAS2 projected on KEGG Metabolic**  
1036 **Pathway.** The map is color coded as in S2 Fig. Highlighted are the DEGs (black lines) and SPMs  
1037 (black dots) for *ras2* integration analysis and gray boxes are used to delineate clusters associated  
1038 with a specific pathway.

1039

1040 **S1 Table. Single-omics analysis results for wildtype between 2% (H) and 0.05% (L) glucose.**  
1041 First block shows GSEA for transcriptomics with adjusted p-value <0.05, arranged in ascending  
1042 order; second block shows MetaboAnalystR pathway enrichment analysis for metabolomics with  
1043 combined p-value <0.05 arranged in ascending order. Reproduced from [13].

1044

1045 **S2 Table.** Results and statistics of transcriptomics, metabolomics and multi -omics integration for  
1046 *gpr1*, each as a separate sheet.

1047

1048 **S3 Table.** Results and statistics of transcriptomics, metabolomics and multi -omics integration for  
1049 *snf3 rgt2*, each as a separate sheet.

1050

1051 **S4 Table.** List of DEGs for each subset of the Venn diagram in Fig 2A.

1052

1053 **S5 Table.** List of SPMs for each subset of the Venn diagram in Fig 3A.

1054

1055 **S6 Table.** In house compound identification.

1056

1057 **S7 Table.** Results and statistics of transcriptomics, metabolomics and multi -omics integration for  
1058 *gpa2*, each as a separate sheet.

1059



1060 **S8 Table.** Results and statistics of transcriptomics, metabolomics and multi -omics integration for  
1061 *ras2*, each as a separate sheet.

1062

1063 **S9 Table.** List of DEGs for each subset of the Venn diagram in Fig 5A.

1064

1065 **S10 Table.** List of SPMs for each subset of the Venn diagram in Fig 6A.

1066

1067 **S11 Table.** List of DEGs for each subset of the Venn diagram in Fig 8A.

1068

1069 **S12 Table.** List of SPMs for each subset of the Venn diagram in Fig 9A

1070

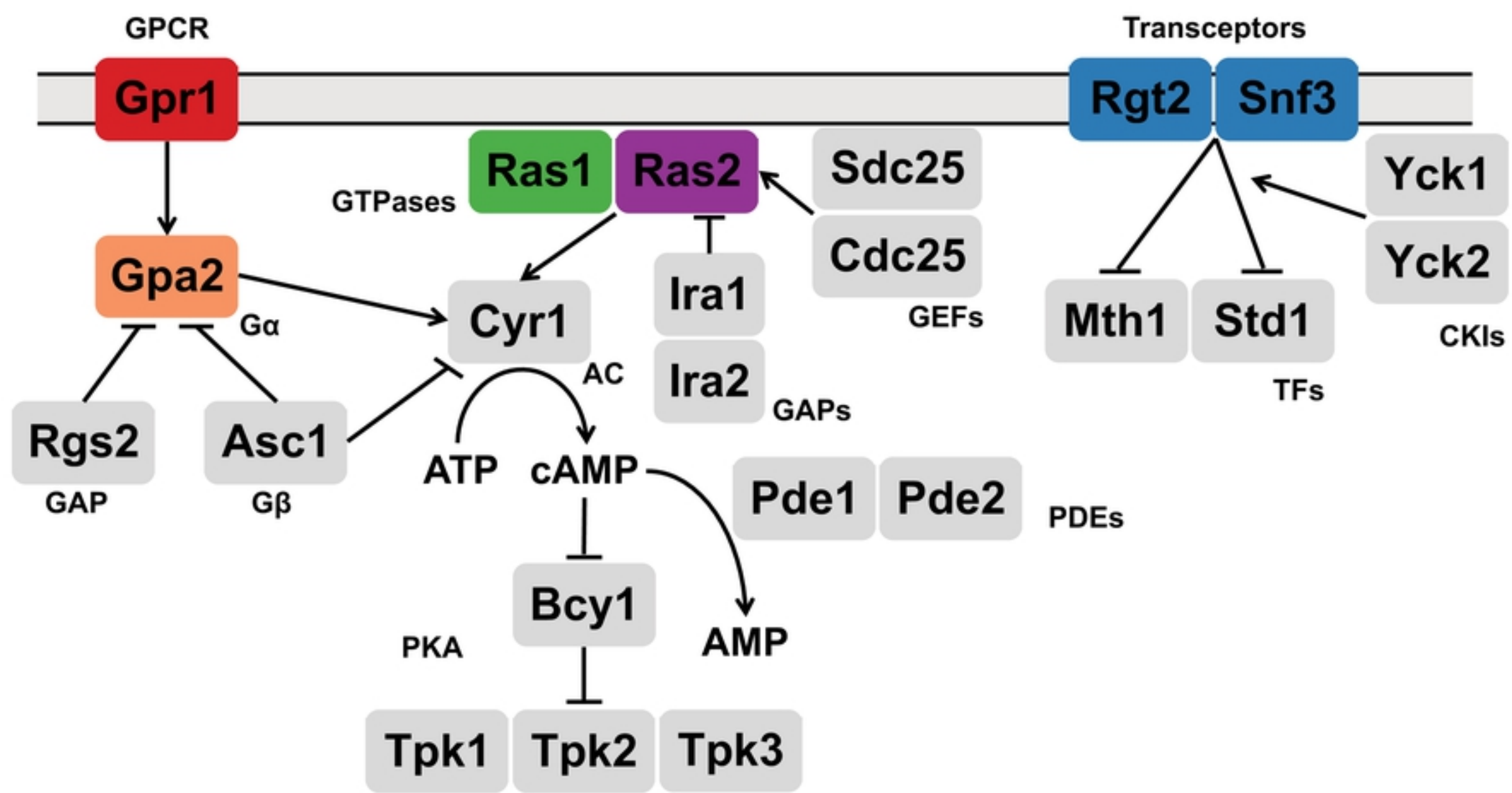
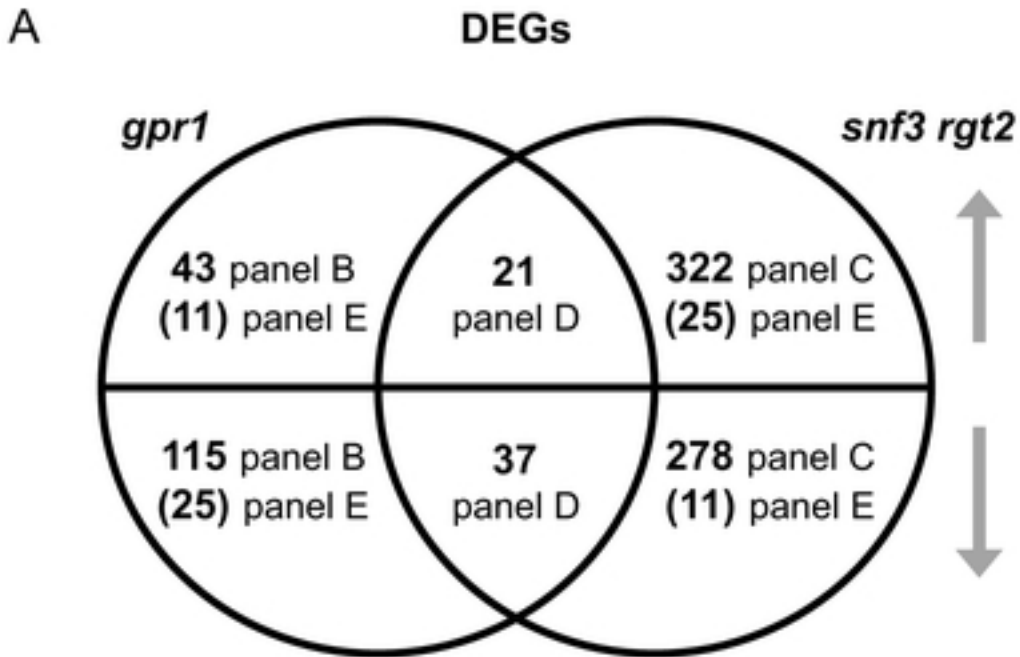


Figure 1



**B**

pathways	adjusted p-value	functional category
Oxidative phosphorylation	5.57E-19	Energy
Starch and sucrose metabolism	9.68E-05	Carbohydrate
Carbon metabolism	0.0151	Carbohydrate
Glycolysis / Gluconeogenesis	0.0213	Carbohydrate
Citrate cycle (TCA cycle)	0.0283	Carbohydrate
Amino sugar and nucleotide sugar metabolism	0.0358	Carbohydrate
Fatty acid metabolism	0.0414	Lipid
Galactose metabolism	0.0422	Carbohydrate
Fatty acid biosynthesis	0.0422	Lipid
Riboflavin metabolism	0.0472	Cofactors and vitamins

**C**

pathways	adjusted p-value	functional category
Ribosome	3.04E-59	Genetic information processing
Longevity regulating pathway	0.0004	Organismal systems
Purine metabolism	0.0005	Nucleotide
Sulfur metabolism	0.0050	Energy
One carbon pool by folate	0.0281	Cofactors and vitamins
Biosynthesis of cofactors	0.0451	Cofactors and vitamins

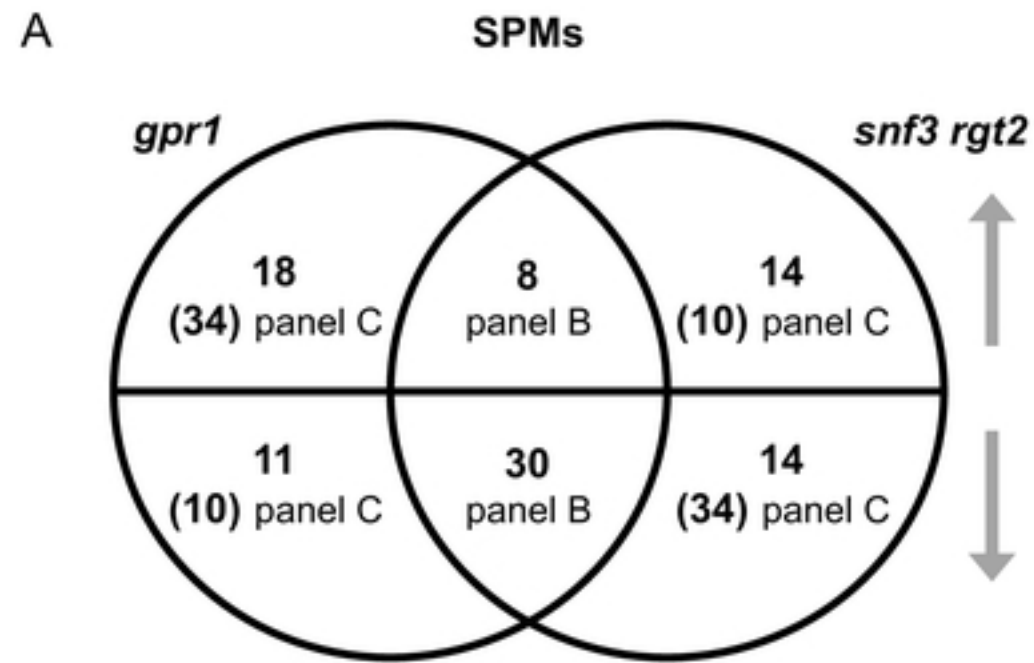
**D**

pathways	adjusted p-value	functional category
Steroid biosynthesis	0.0332	Lipid
Biosynthesis of amino acids	0.0380	Amino acid
Nitrogen metabolism	0.0392	Energy

**E**

pathways	adjusted p-value	functional category
Pyruvate metabolism	0.0137	Carbohydrate
Glycolysis / Gluconeogenesis	0.0137	Carbohydrate
Carbon metabolism	0.0152	Carbohydrate
Citrate cycle (TCA cycle)	0.0152	Carbohydrate
Ascorbate and aldarate metabolism	0.0231	Carbohydrate
beta-Alanine metabolism	0.0236	Carbohydrate
Valine, leucine and isoleucine degradation	0.0236	Amino acid
Histidine metabolism	0.0236	Amino acid
Lysine degradation	0.0274	Amino acid
Fatty acid degradation	0.0348	Lipid
Tryptophan metabolism	0.0348	Amino acid
Arginine and proline metabolism	0.0386	Amino acid
Pantothenate and CoA biosynthesis	0.0386	Cofactors and vitamins

Figure2



**B**

pathways	adjusted p-value	functional category
Purine metabolism	3.19E-06	Nucleotide

**C**

pathways	adjusted p-value	functional category
Fructose and mannose metabolism	9.16E-05	Carbohydrate
Amino sugar and nucleotide sugar metabolism	0.0003	Carbohydrate

Figure3

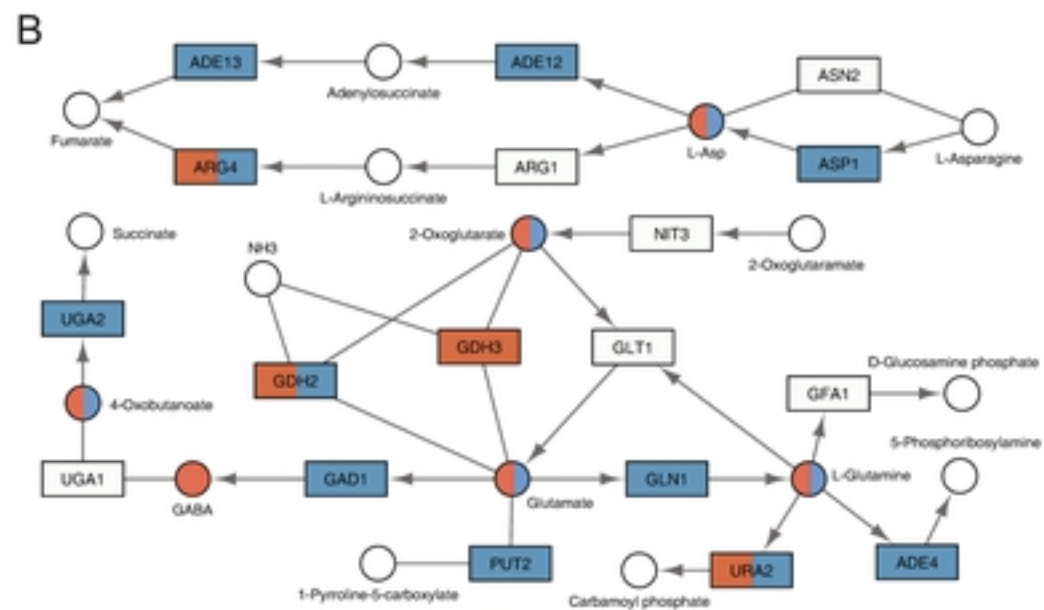
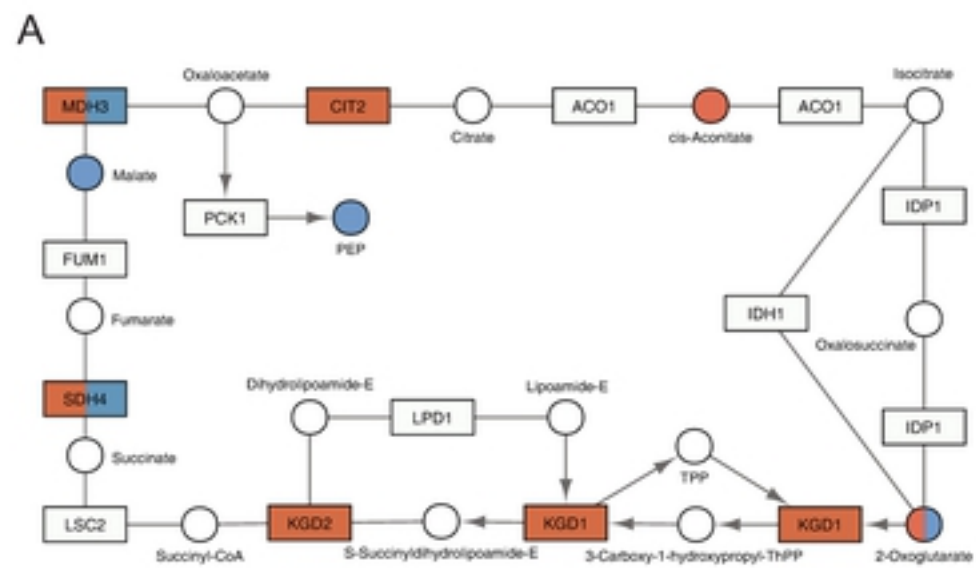
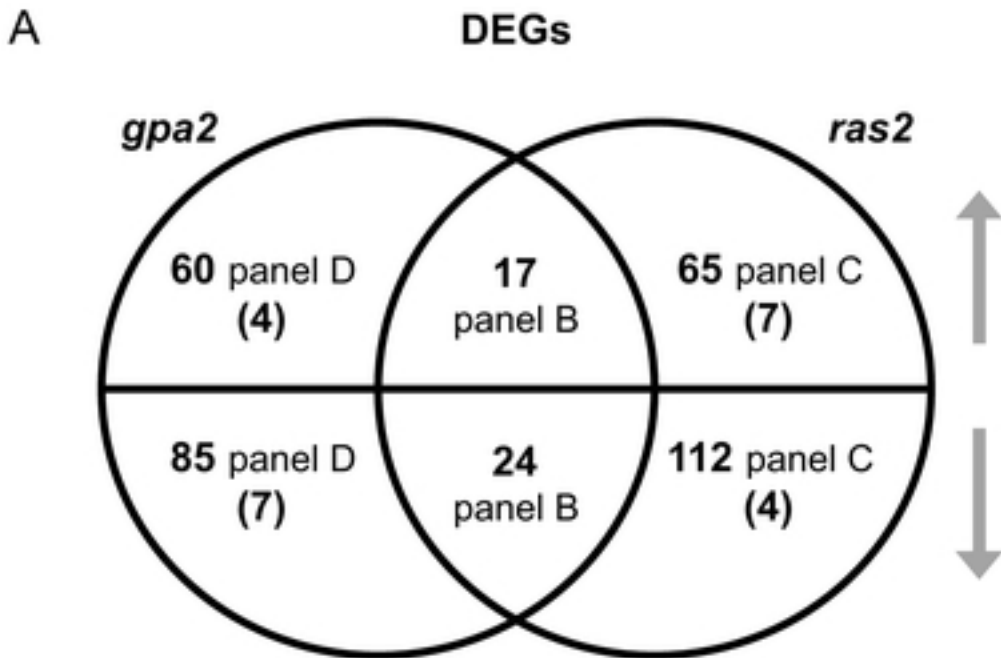


Figure 4



**B**

pathways	adjusted p-value	functional category
Starch and sucrose metabolism	0.0221	Carbohydrate
Histidine metabolism	0.0221	Amino acid
Pyruvate metabolism	0.0221	Carbohydrate
Carbon metabolism	0.0221	Carbohydrate
Glycolysis / Gluconeogenesis	0.0221	Carbohydrate
Fatty acid degradation	0.0258	Lipid
Tryptophan metabolism	0.0258	Amino acid
Arginine and proline metabolism	0.0298	Amino acid
Pentose phosphate pathway	0.0389	Carbohydrate

**C**

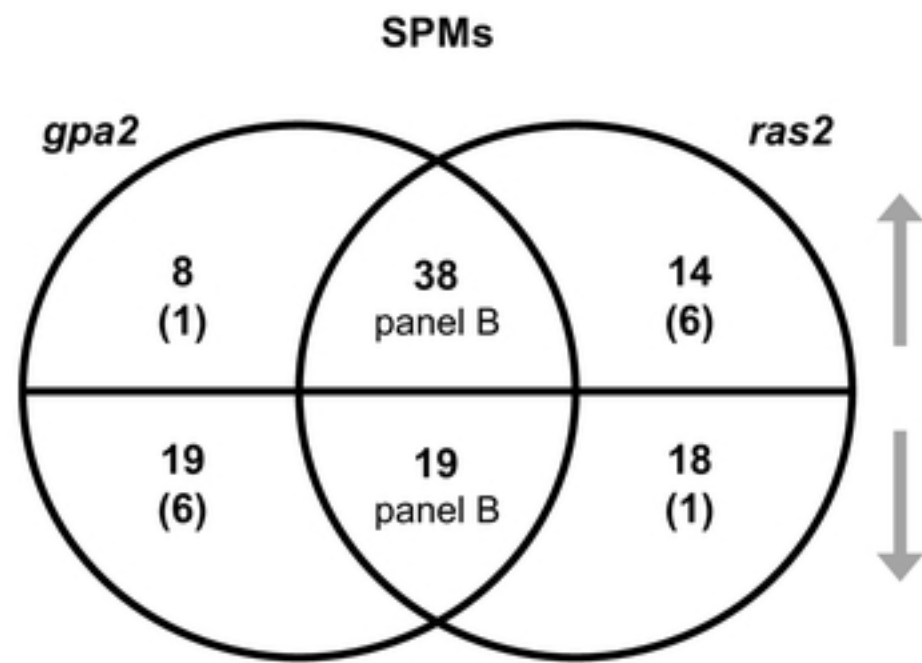
pathways	adjusted p-value	functional category
Carbon metabolism	0.0019	Carbohydrate
Starch and sucrose metabolism	0.0020	Carbohydrate
Nitrogen metabolism	0.0020	Energy
Glycine, serine and threonine metabolism	0.0080	Amino acid
Cysteine and methionine metabolism	0.0080	Amino acid
Biosynthesis of amino acids	0.0128	Amino acid
Methane metabolism	0.0165	Energy
Biosynthesis of cofactors	0.0165	Cofactors and vitamins
Peroxisome	0.0173	Cellular processes
Purine metabolism	0.0221	Nucleotide
Fatty acid degradation	0.0271	Lipid
Galactose metabolism	0.0473	Carbohydrate
Vitamin B6 metabolism	0.0473	Cofactors and vitamins

**D**

pathways	adjusted p-value	functional category
Oxidative phosphorylation	2.23E-16	Energy
Citrate cycle (TCA cycle)	0.0233	Carbohydrate
Fatty acid metabolism	0.0394	Lipid
Fatty acid biosynthesis	0.0474	Lipid

Figure5

A

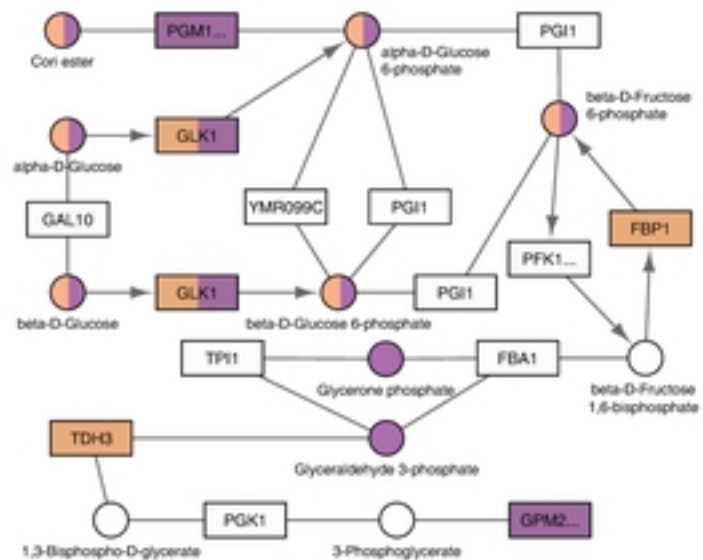


B

pathways	adjusted p-value	functional category
Galactose metabolism	2.09E-08	Carbohydrate
Amino sugar and nucleotide sugar metabolism	9.02E-08	Carbohydrate
Fructose and mannose metabolism	1.01E-05	Carbohydrate
Starch and sucrose metabolism	0.0033	Carbohydrate
Glycolysis / Gluconeogenesis	0.0442	Carbohydrate

Figure6

A



B

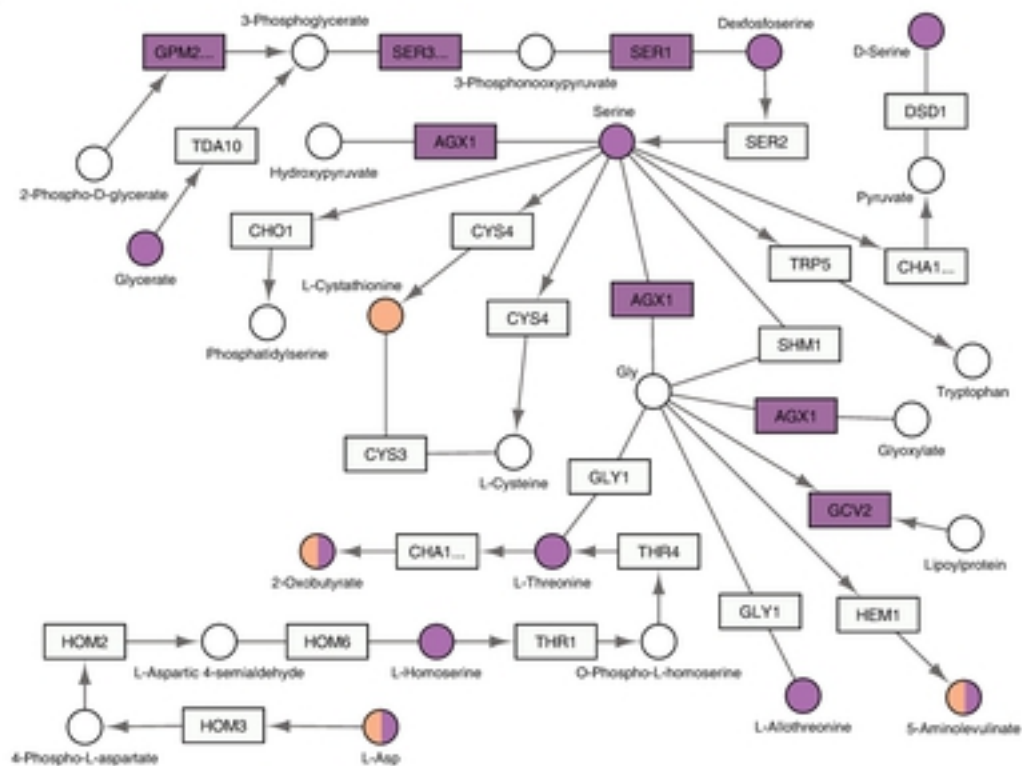
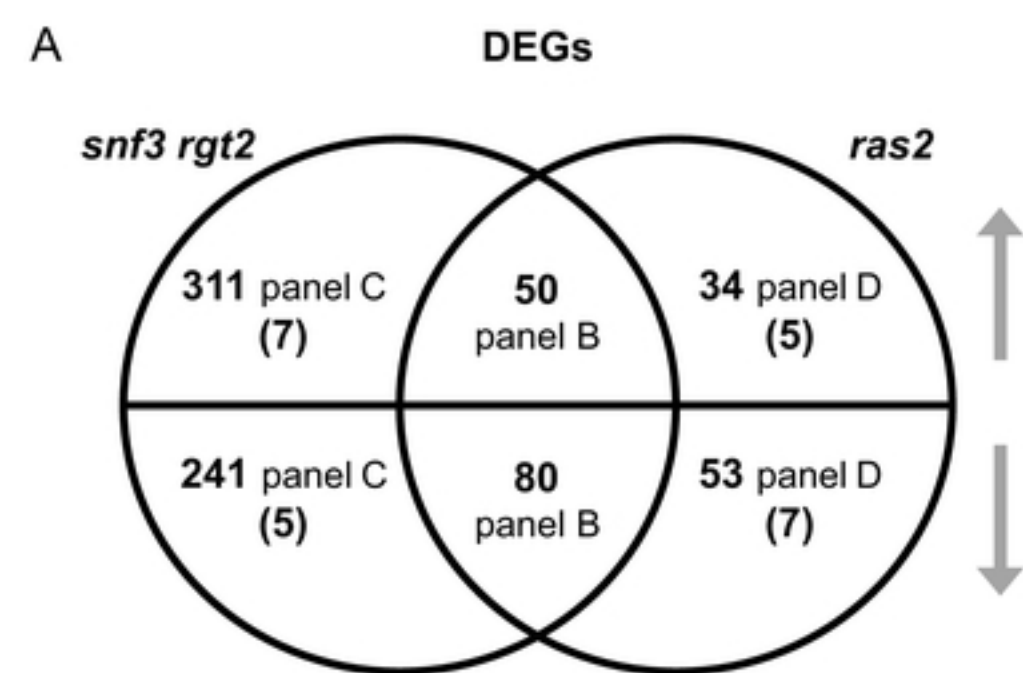


Figure7





**B**

pathways	adjusted p-value	functional category
Nitrogen metabolism	0.0019	Energy
Biosynthesis of amino acids	0.0023	Amino acid
Glycine, serine and threonine metabolism	0.0023	Amino acid
Methane metabolism	0.0080	Energy
Carbon metabolism	0.0089	Carbohydrate
Cysteine and methionine metabolism	0.0089	Amino acid
Biosynthesis of cofactors	0.0231	Cofactors and vitamins
Vitamin B6 metabolism	0.0331	Cofactors and vitamins
Sulfur metabolism	0.0450	Energy

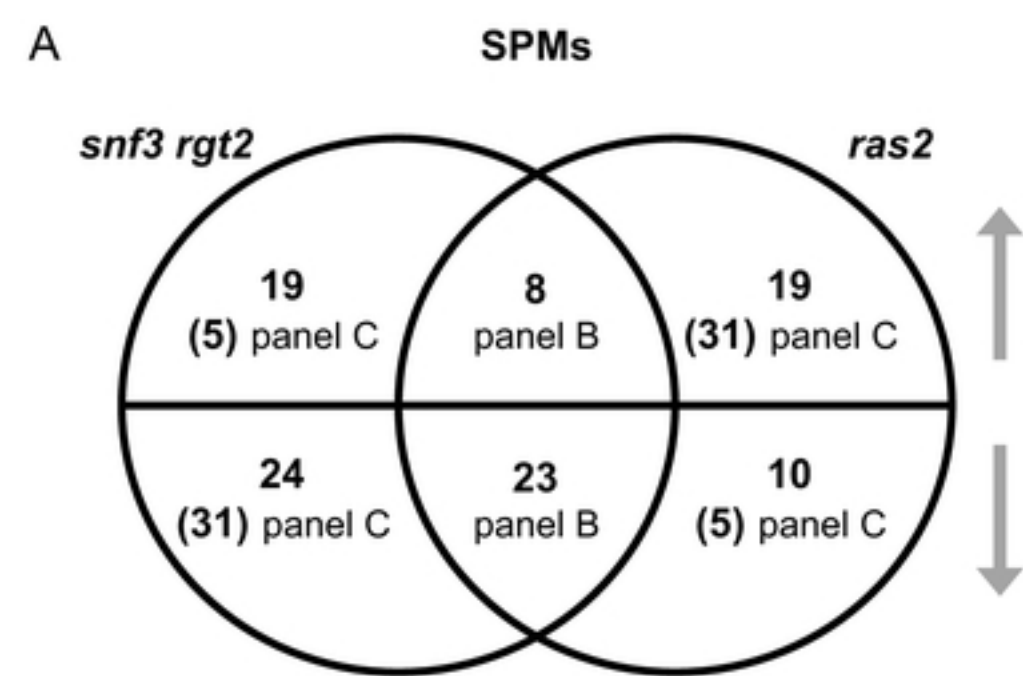
**C**

pathways	adjusted p-value	functional category
Ribosome	1.75E-56	Genetic information processing
Purine metabolism	0.0008	Nucleotide
Longevity regulating pathway	0.0020	Organismal systems

**D**

pathways	adjusted p-value	functional category
Starch and sucrose metabolism	5.15E-08	Carbohydrate
Carbon metabolism	2.66E-05	Carbohydrate
Galactose metabolism	0.0002	Carbohydrate
Glyoxylate and dicarboxylate metabolism	0.0003	Carbohydrate
Amino sugar and nucleotide sugar metabolism	0.0006	Carbohydrate
Pentose phosphate pathway	0.0030	Carbohydrate
Citrate cycle (TCA cycle)	0.0038	Carbohydrate
Glutathione metabolism	0.0160	Amino acid
Glycolysis / Gluconeogenesis	0.0252	Carbohydrate

Figure8



**B**

pathways	adjusted p-value	functional category
Purine metabolism	0.0002	Nucleotide
Alanine, aspartate and glutamate metabolism	0.0243	Amino acid

**C**

pathways	adjusted p-value	functional category
Amino sugar and nucleotide sugar metabolism	0.0001	Carbohydrate
Fructose and mannose metabolism	0.0003	Carbohydrate

Figure9

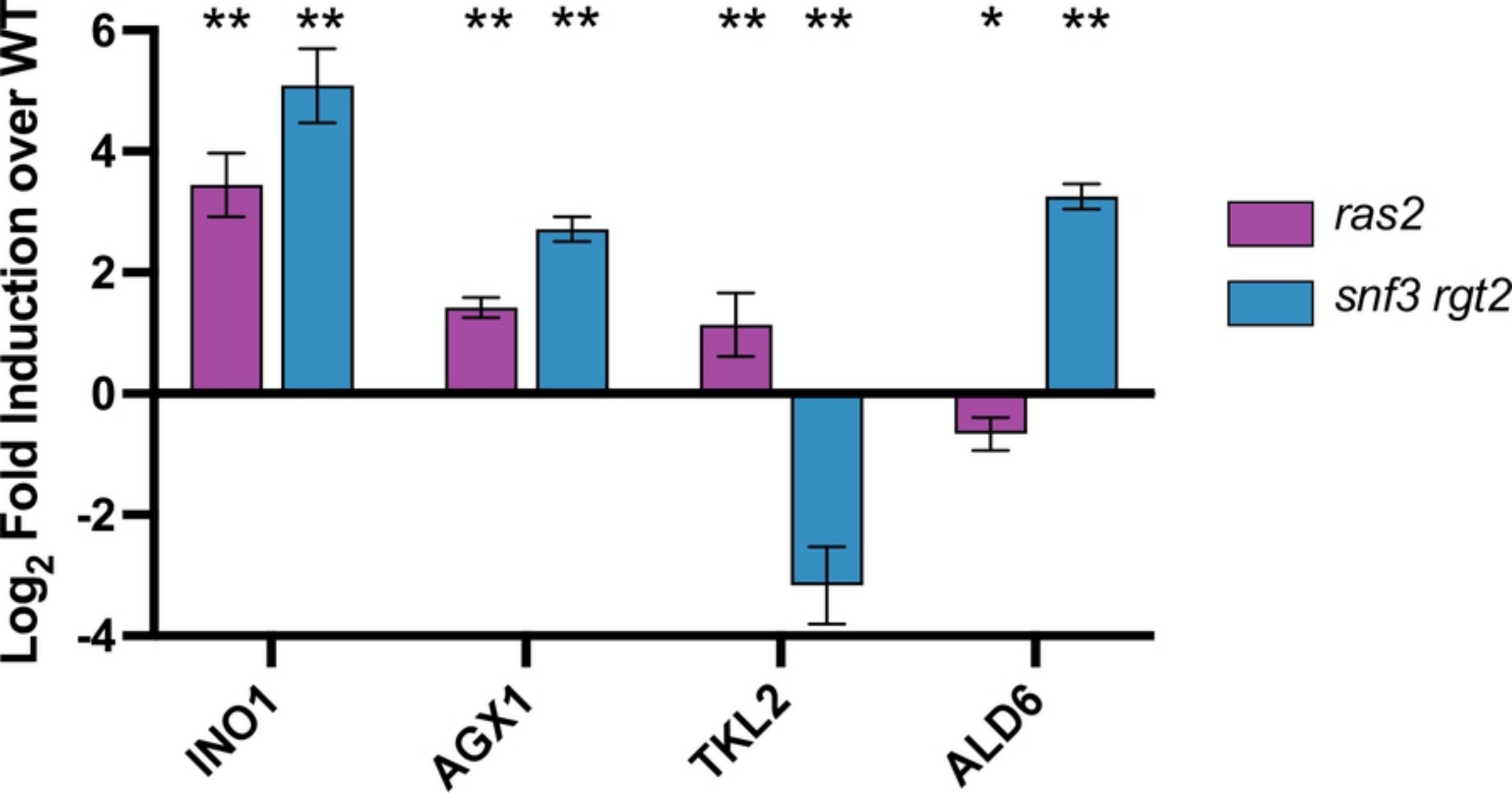


Figure10